Exceptional service in the national interest

SAND2016-1490C

Sandia National Laboratories

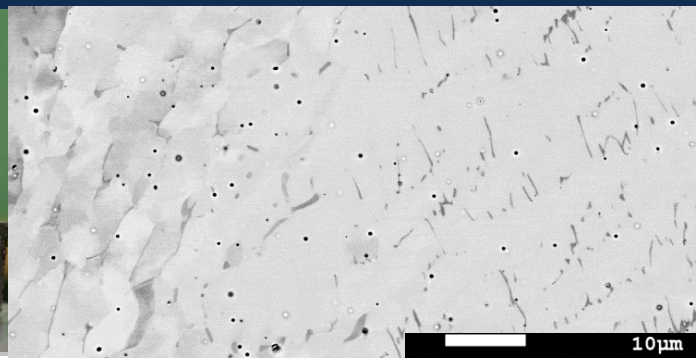

Microstructure and Mechanical Property Relationships in Additively Manufactured 304L

Mike Maguire, Jeff Rodelas, Joe Michael, Dave Adams, Jay Carroll, Bo Song, Ben Reedlunn, Joe Bishop, and Jack Wise

Sandia National Laboratories

Todd Palmer

Applied Research Laboratory, Pennsylvania State University

TMS 2016, February 14-18, Nashville, TN

Sandia National Laboratories is a multi-program laboratory managed and operated by Sandia Corporation, a wholly owned subsidiary of Lockheed Martin Corporation, for the U.S. Department of Energy's National Nuclear Security Administration under contract DE-AC04-94AL85000. SAND 2015-5700A

Sandia California

Sandia National Laboratories

View out our front door

Sandia California

View out our back door

Topics

- Summary of SNL project to characterize additively manufactured 304L using Direct Energy Deposition (DED) processes (mechanical testing and direct numerical simulation of deformation)
- Microstructure and mechanical property results
  - Variability of DED results vs. wrought bar
- Discussion of why the results are what they are:
  - Solidification metallurgy
  - Microchemistry of deposits
  - Relative contribution of strengthening mechanisms

Project envisioned to characterize AM 304L over multiple decades of strain rate

Sandia National Laboratories

Quasistatic 10^{-5} – 10^{0}

Crystal Plasticity Modeling

Dynamic 5×10^{2} – 3×10^{3} s^{-1}

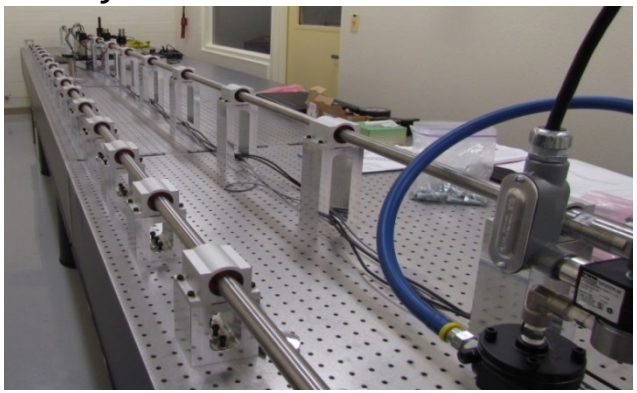

Plate Impact 10^{7} – 10^{9} s^{-}

Microscopy and Analytical Microsopy

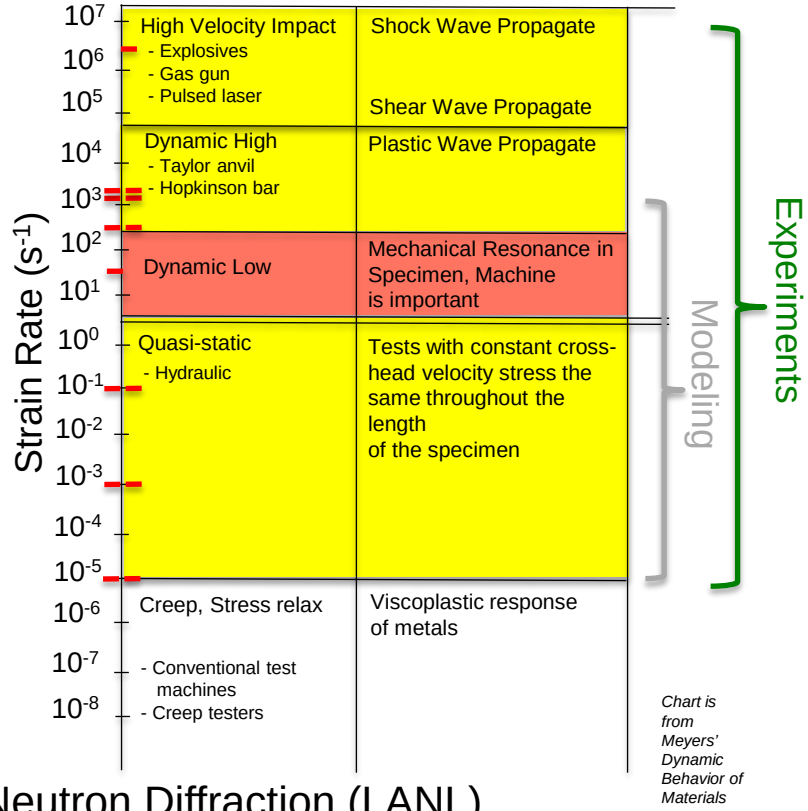

Neutron Diffraction (LANL)

Mechanical Testing Plan

- Comparison with wrought SS304L
- Example compression and tension samples
  - Static tension and compression ($\dot{\epsilon}$ = 10^{0} to 10^{-5}) – *Jay Carroll*
  - Kolsky bar tension ($\dot{\epsilon}$ = 500, 1500, 2500 s^{-1}) – *Bo Song*
  - Gas gun ($\dot{\epsilon} \approx 10^{7}$ s^{-1}) – *Jack Wise*
- ASTM geometries chosen, when possible
- Test samples removed by wire EDM, then machined
- Tests probe variability from within DED deposit
- Sampling Plan had over 1000 tests planned

Sample Preparation

- **Laser Power & Process**
  - **Power (2.0 kW, 3.8 kW)**
  - **Parallel hatch vs. Cross Hatch**
  - **Varying test direction w.r.t. process orientation**

- **Issues**
  - **Anisotropy**
    - **X direction**
    - **Y direction**
    - **Z direction**
  - **Residual Stress**
    - **Annealing vs. as-deposited**

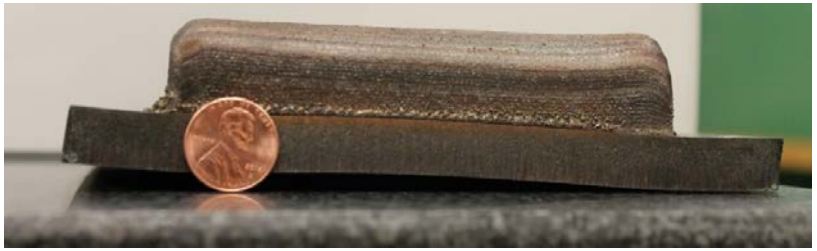

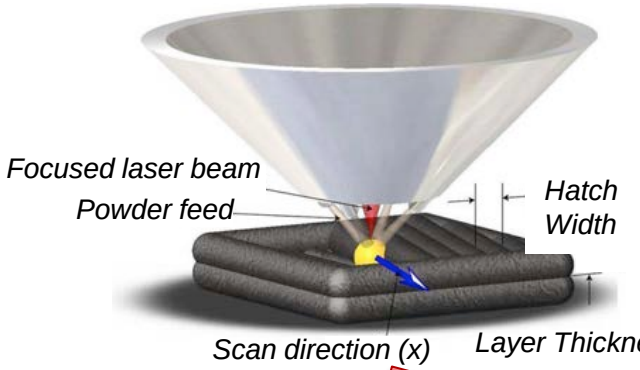

Used DED to produce 2.5 x 2.5 x 10 cm blocks

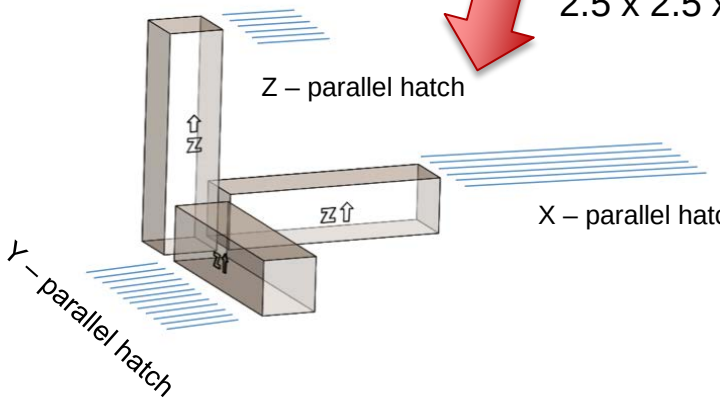

3.8 kW

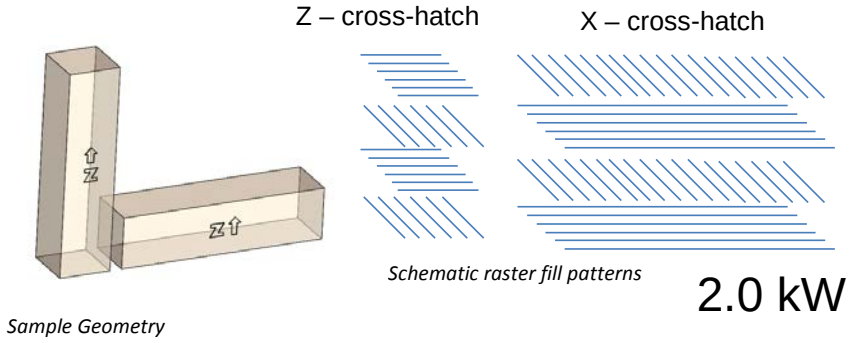

2.0 kW

Directed Energy Deposition (DED) at ARL

Sandia National Laboratories

Build parameters (Schema) developed by T. Palmer, ARL

Laser Power (W) 4 mm spot size	Travel Speed (mm/min)	Powder Feed Rate (g/min)	Hatch Spacing (mm)	Layer Thickness (mm)
2000	508	20	2	0.89
3800	508	23	2	1.25

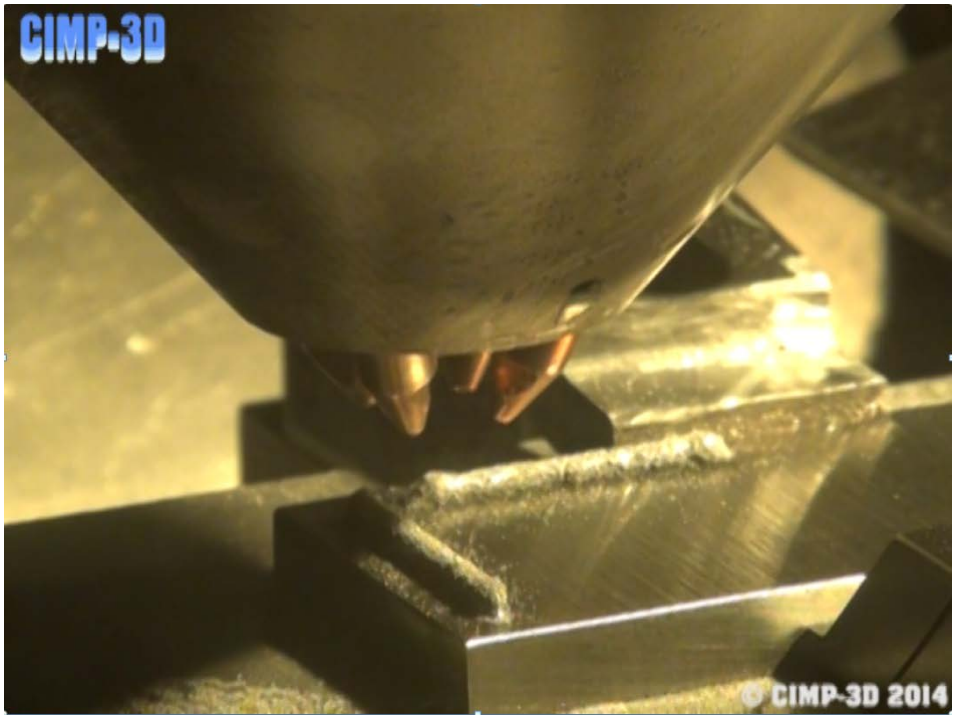

SNL LENS™ housing (ca. 2000)

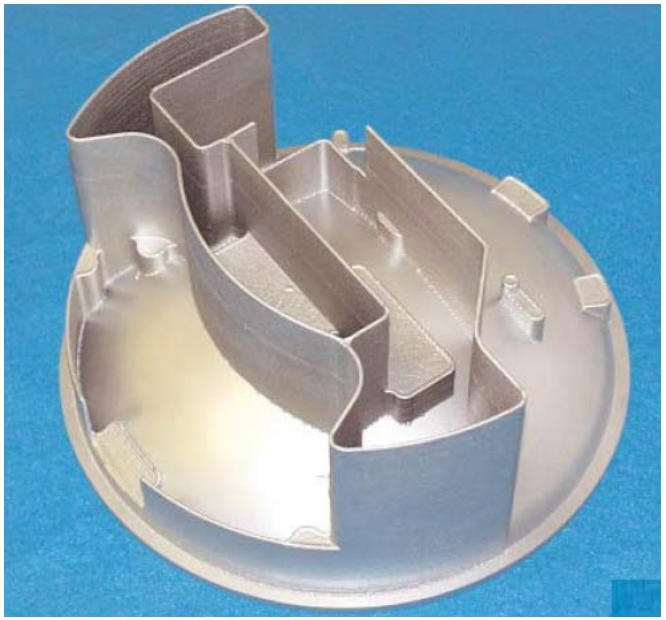

Sample Blocks Prepared by ARL

6 in. 6 in. x 0.5 in. 304 starter plate
Carpenter MicroMelt 304L Powder (44-105 μm)

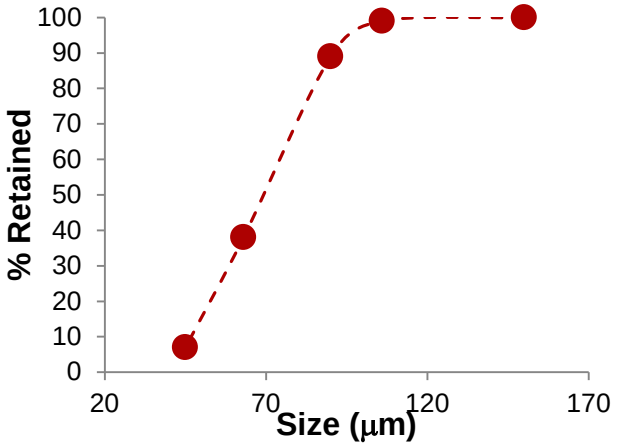

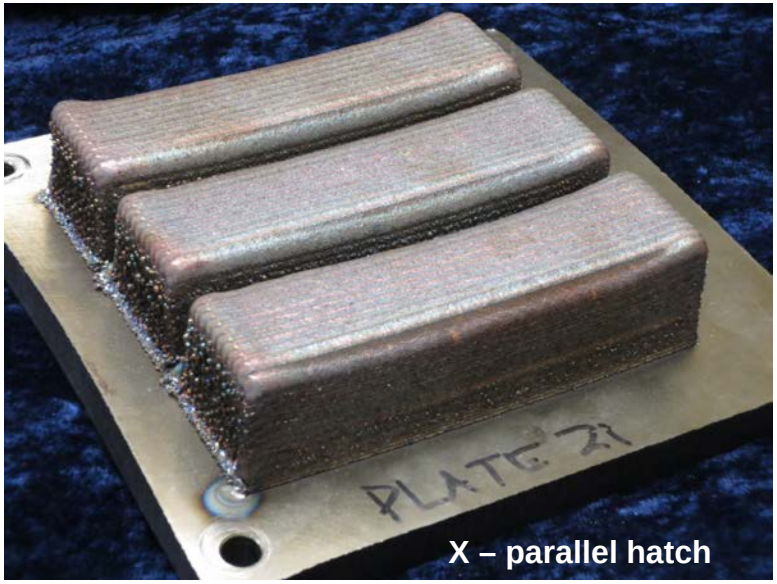

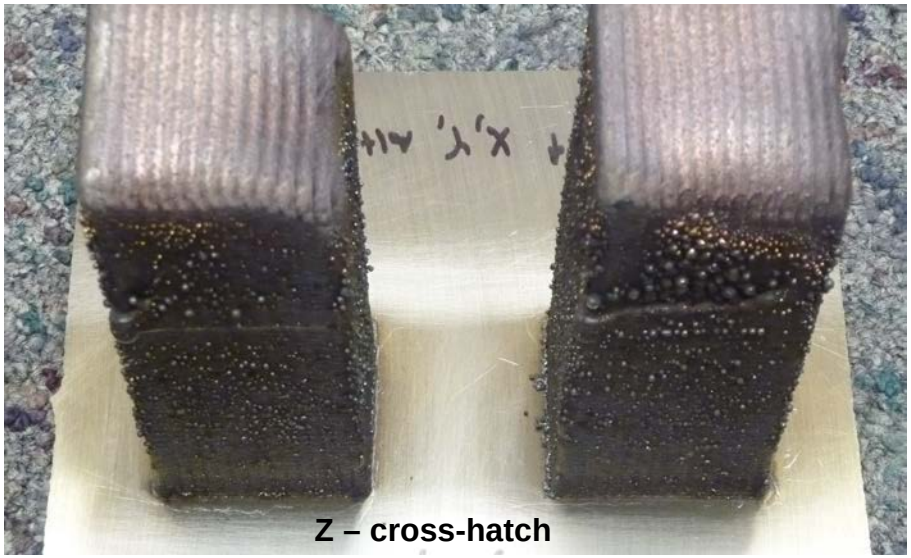

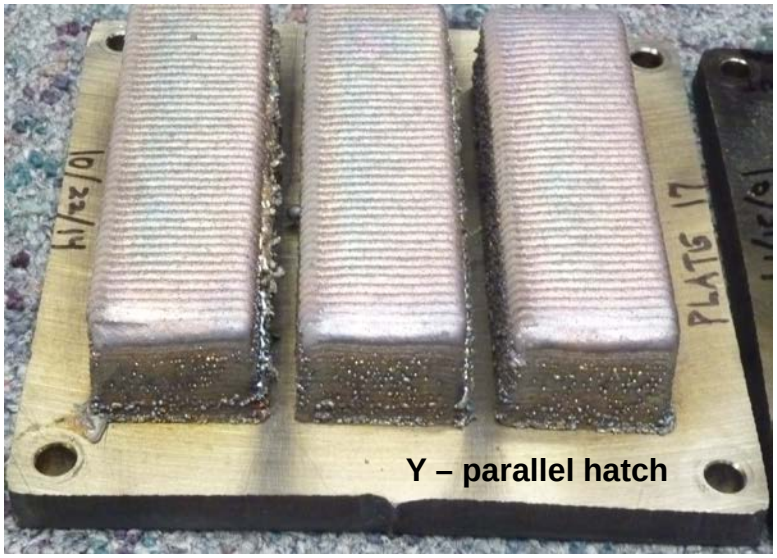

Elemental Changes During Deposition

Initial Powder Composition:

Cr	Ni	Mn	Si	Mo	Cu	N	P	C	S	O
19.07	10.38	1.55	0.50	0.04	0.03	0.089	0.009	0.013	0.006	0.017

ICP/OES + Leco gas fusion

Cr, Ni, Mn, N, and C

Si, P, S, O

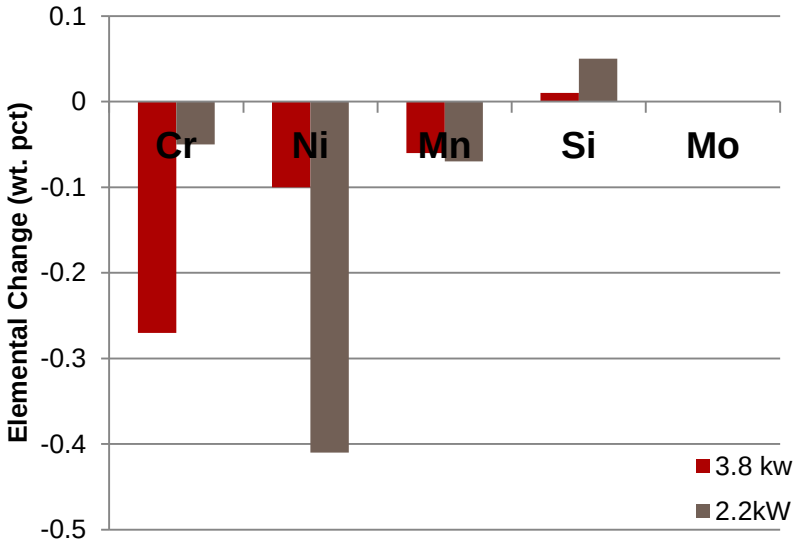

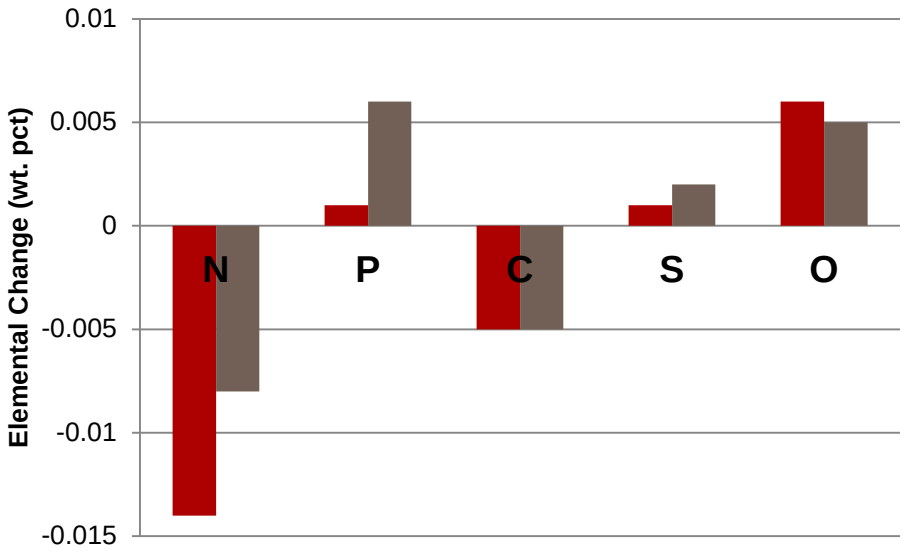

Large area views of microstructure of AM SS304L (2.0 kW)

- **Electron backscatter diffraction maps of electropolished surface.**
- **Example shown to right was built with a cross hatch approach.**
- **Density has been confirmed at 99.85% FTD (Archimedes method).**

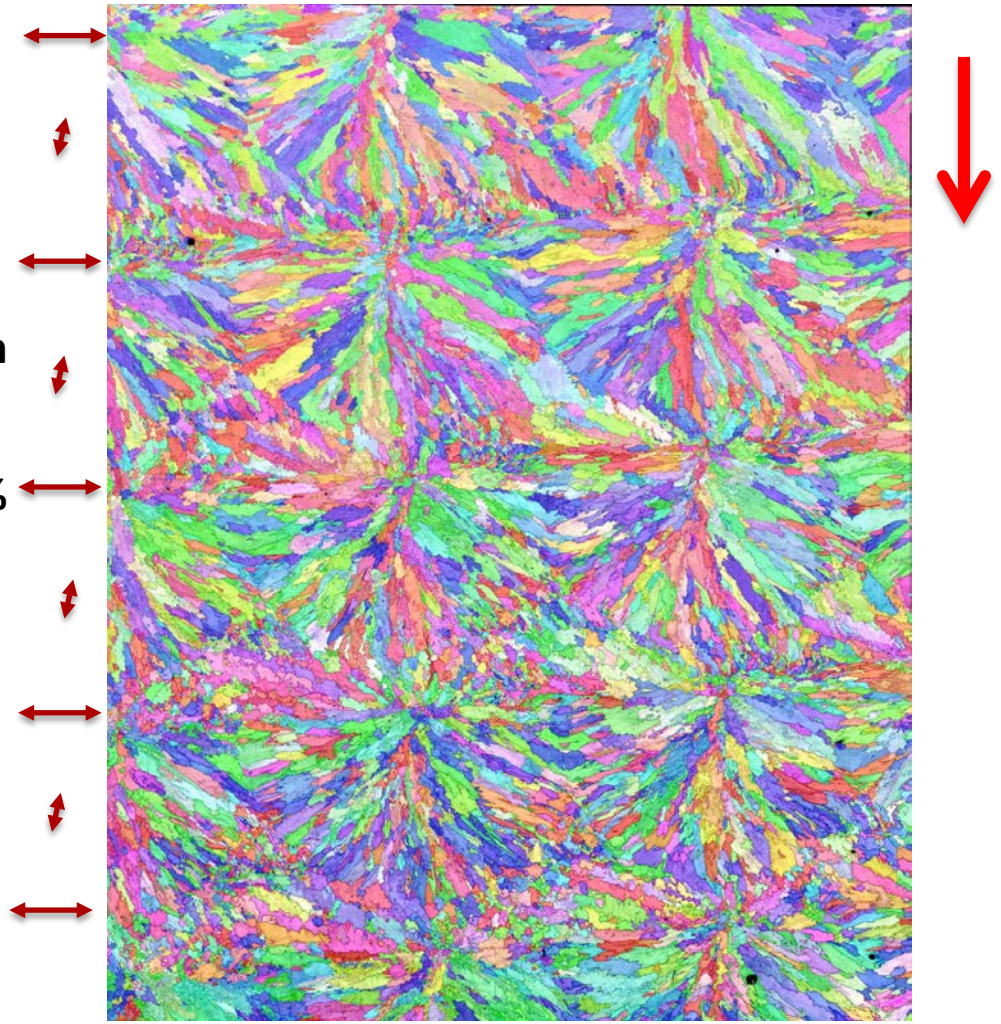

IPF X + BC

6 mm wide by 10 mm high

DED material is significantly stronger than wrought bar but exhibits less ductility

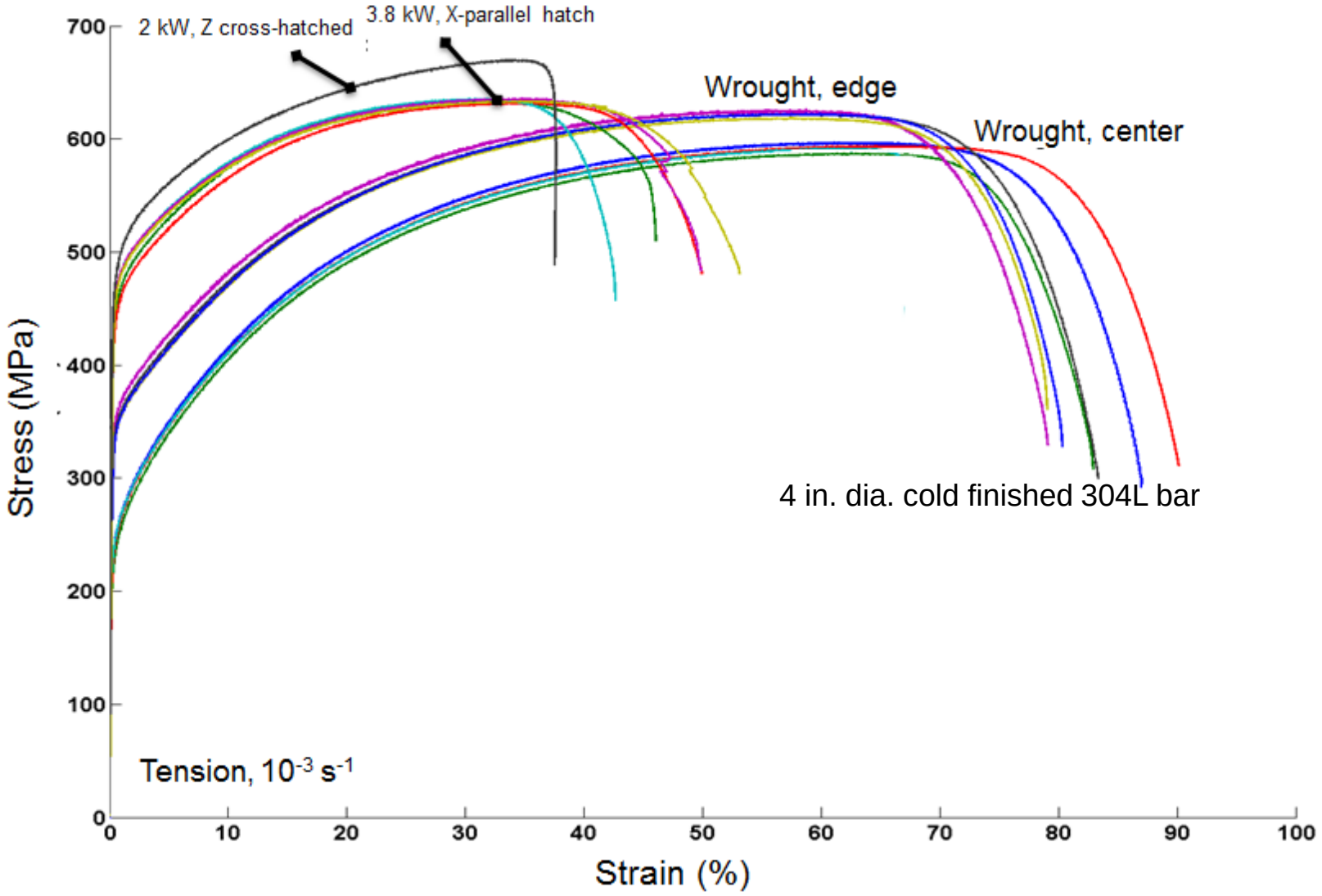

Summary of DED static tensile data

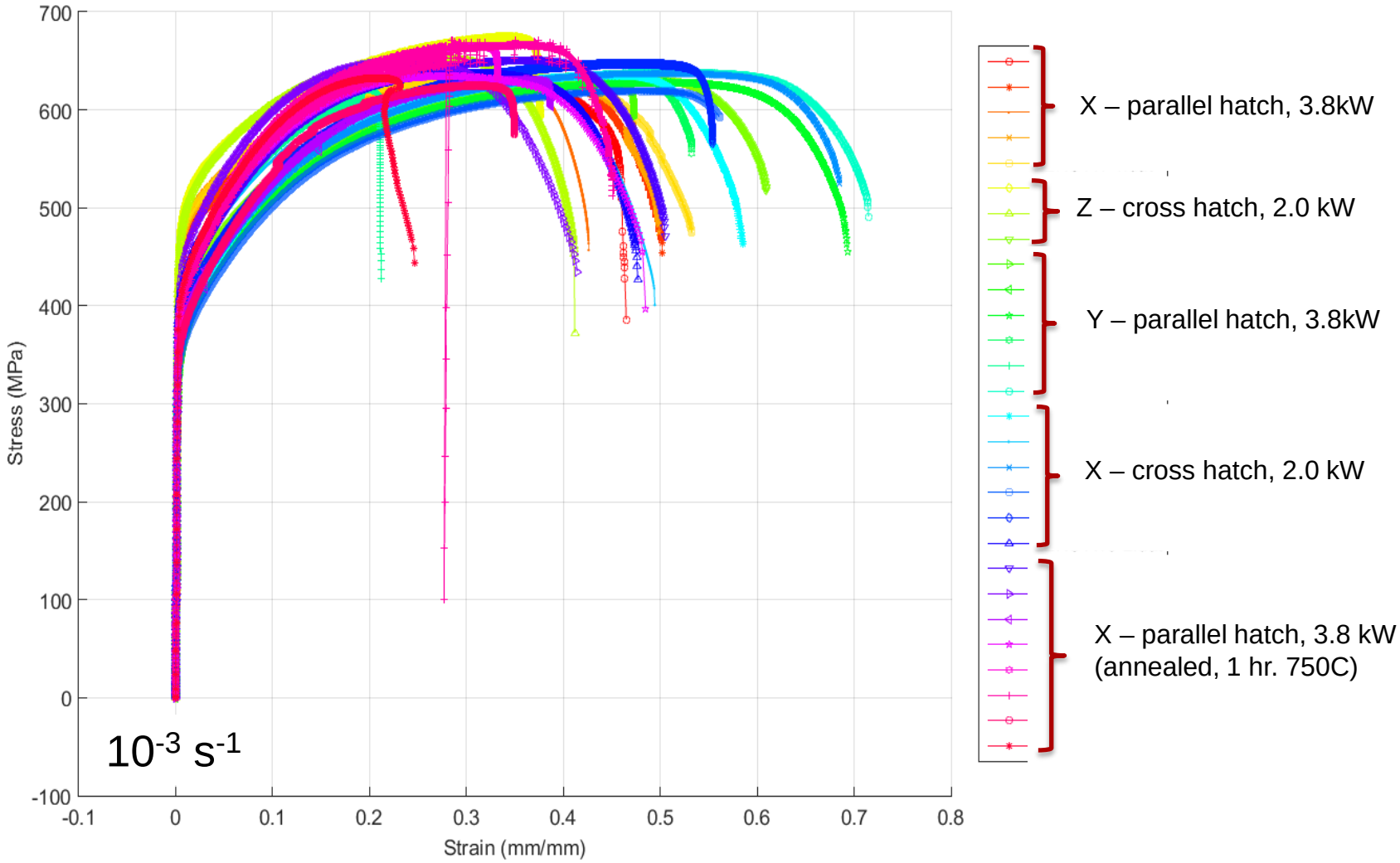

Variability of mechanical properties is large, but not hopeless to characterize …

Summary of DED static tensile data

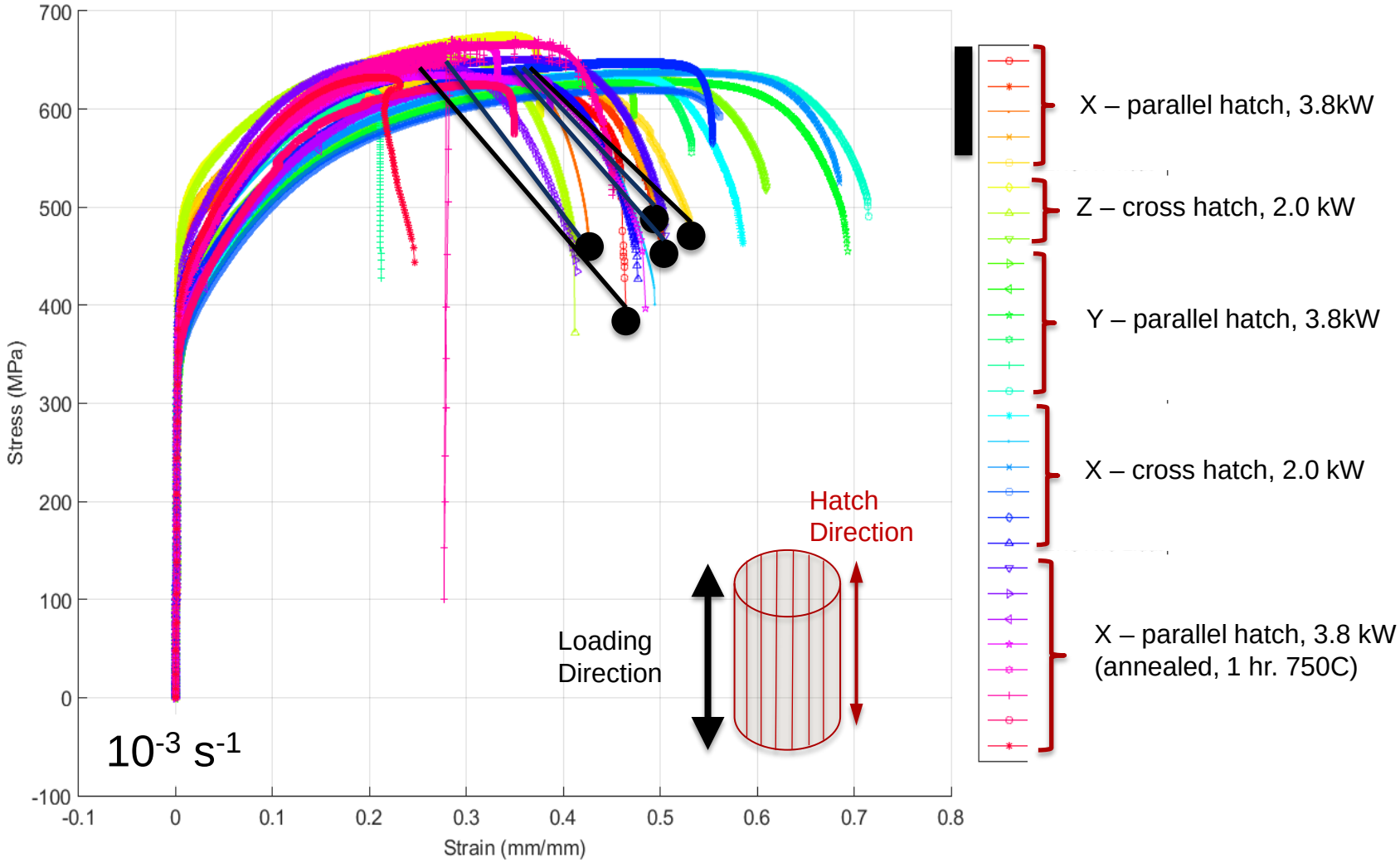

Summary of DED static tensile data

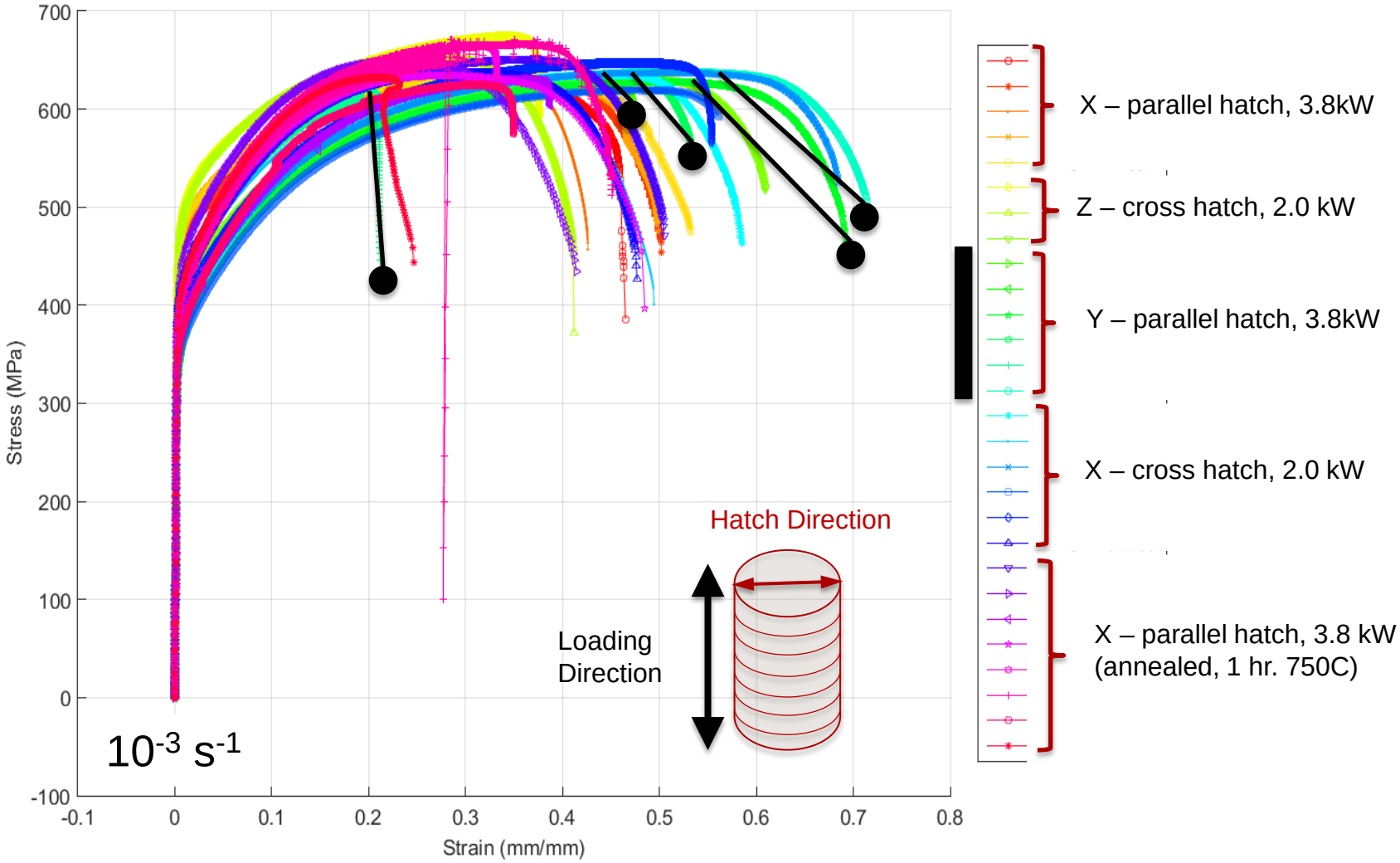

Wider observed variability in ductility with this orientation

Summary of DED static tensile data

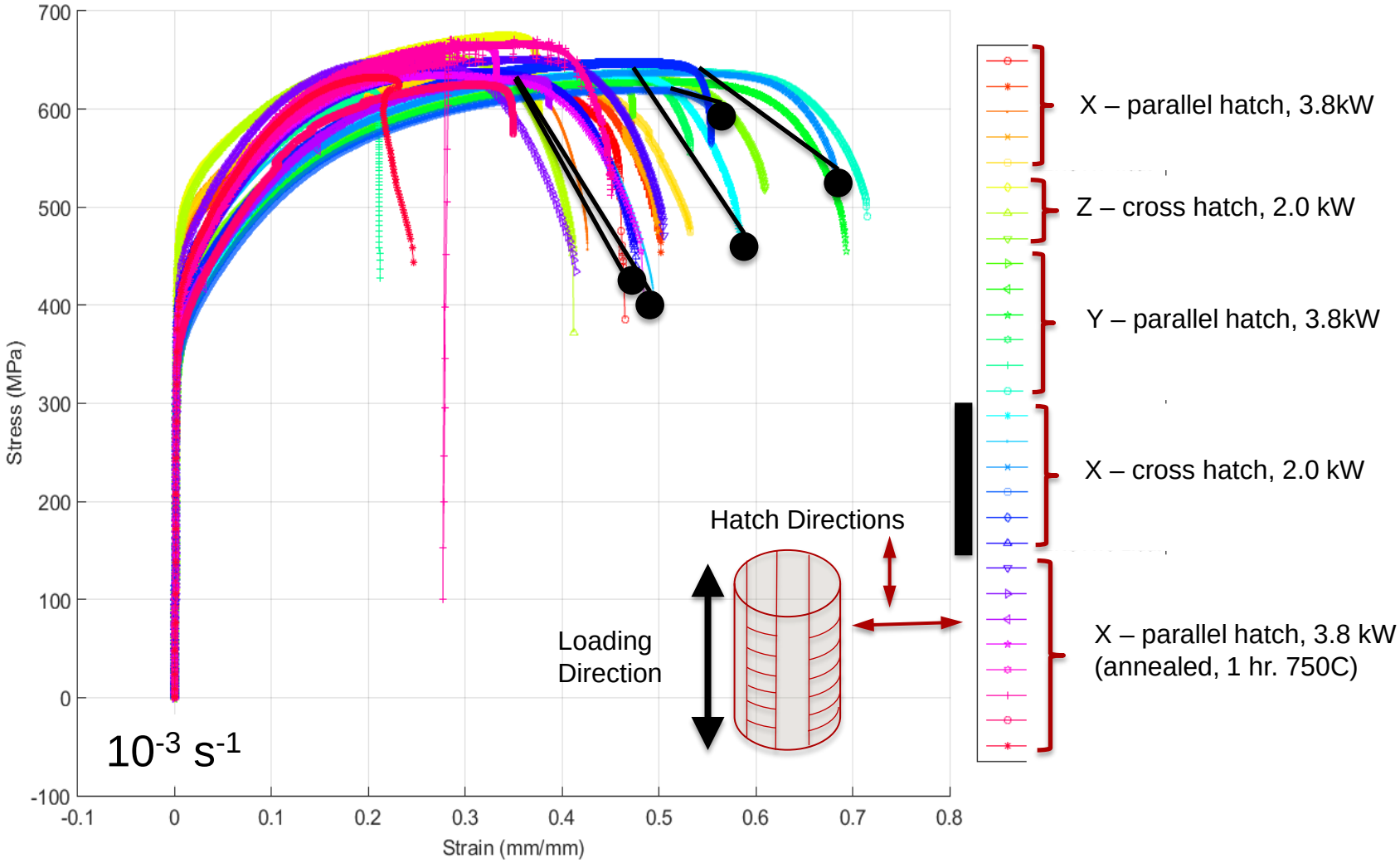

Kolsky Bar Compression at 500 and 2500 s^{-1}

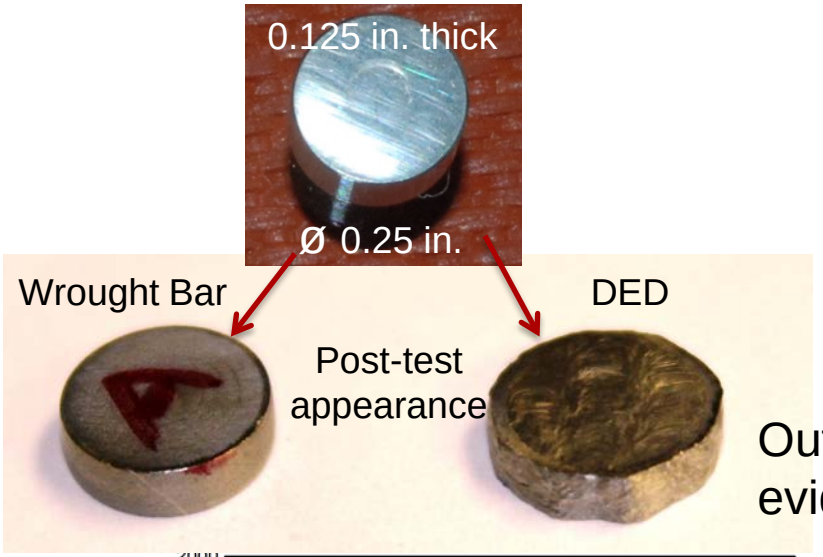

- DED material shows higher flow stresses than 304L wrought bar below $\varepsilon = 0.3$
- Wrought material shows higher strain hardening rate above $\varepsilon = 0.15$
- Positional effects (edge vs. center) not evident (residual stresses likely eliminated by sectioning)
- 2.2 kW deposit shows higher flow stress than 3.8 kW deposit

Outline of deposit puddles are evident in sample after testing

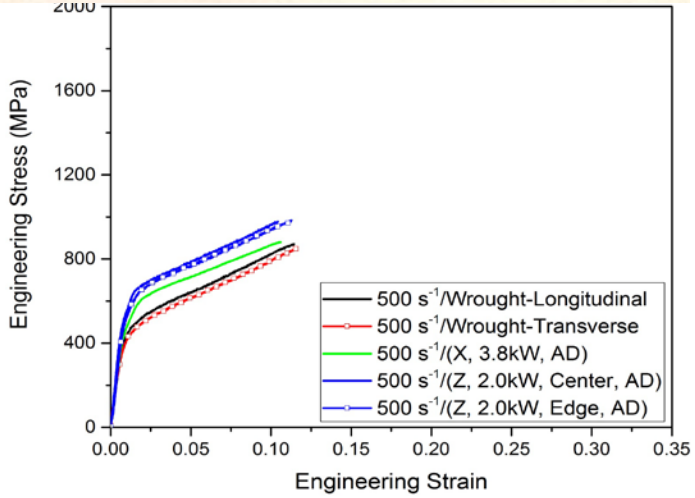

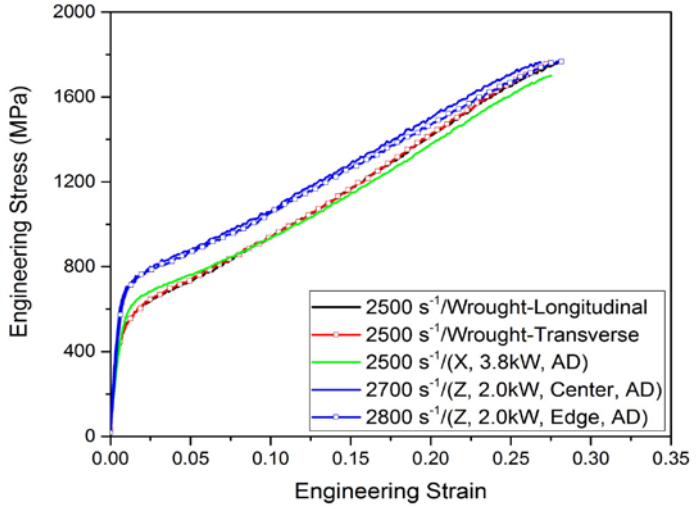

Tension results at 2500 s^{-1}

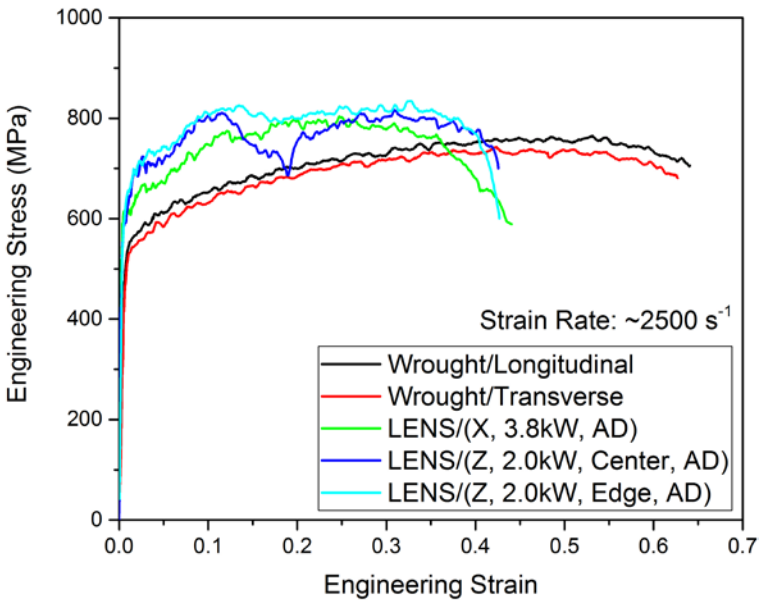

Tension results show:

- Higher flow stress
- Less ductility in DED material
- Coarse, mottled appearance after deformation, similar to compression samples

DED Deposit

Wrought Bar

High strain rate impact experiments have been completed.

Utilizes Sandia's DICE/Veloce laboratory (J. Wise)

- Reverse Ballistic Impact Tests
  - DED or wrought SS304L impacting LiF, Al_2O_3, PMMA at v = 80, 200, 350 m/s (up to 60 kbar)
  - Uniaxial strain test
  - **Determines Hugoniot stress-strain relationship**

- Forward Ballistic Impact Tests
  - Sapphire impacting LENS (x and y), wrought SS304L
  - Speeds of 80, 200, 350 m/s (up to 60 kbar)
  - **Hugoniot elastic limit (HEL) determination**

- Forward Ballistic:
  - Sapphire impacting LENS (x and y), wrought SS304L
  - Speeds to be determined
  - **Spall strength tests**

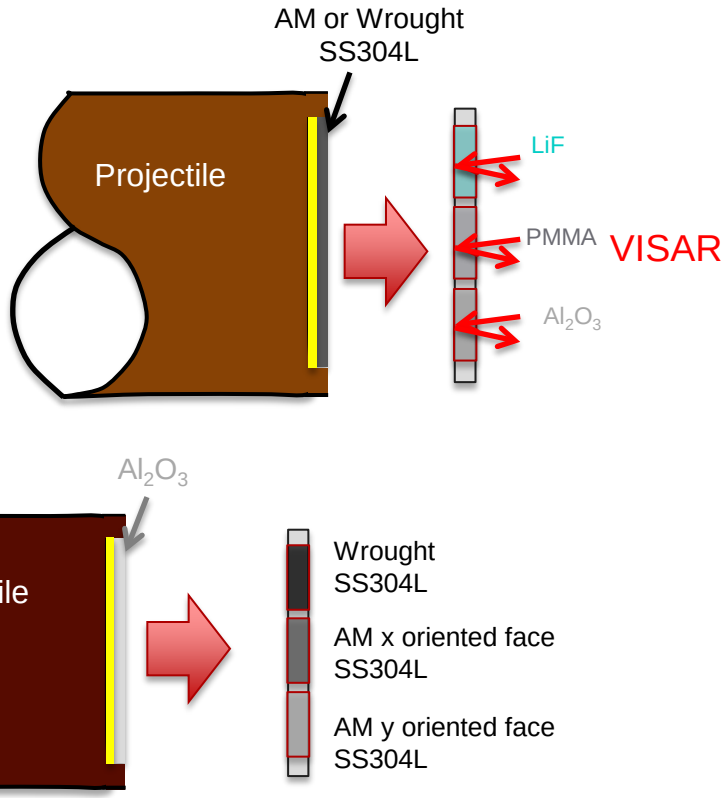

Reverse Ballistic Tests: Hugoniot Results for DED (3.8 kW) Stainless

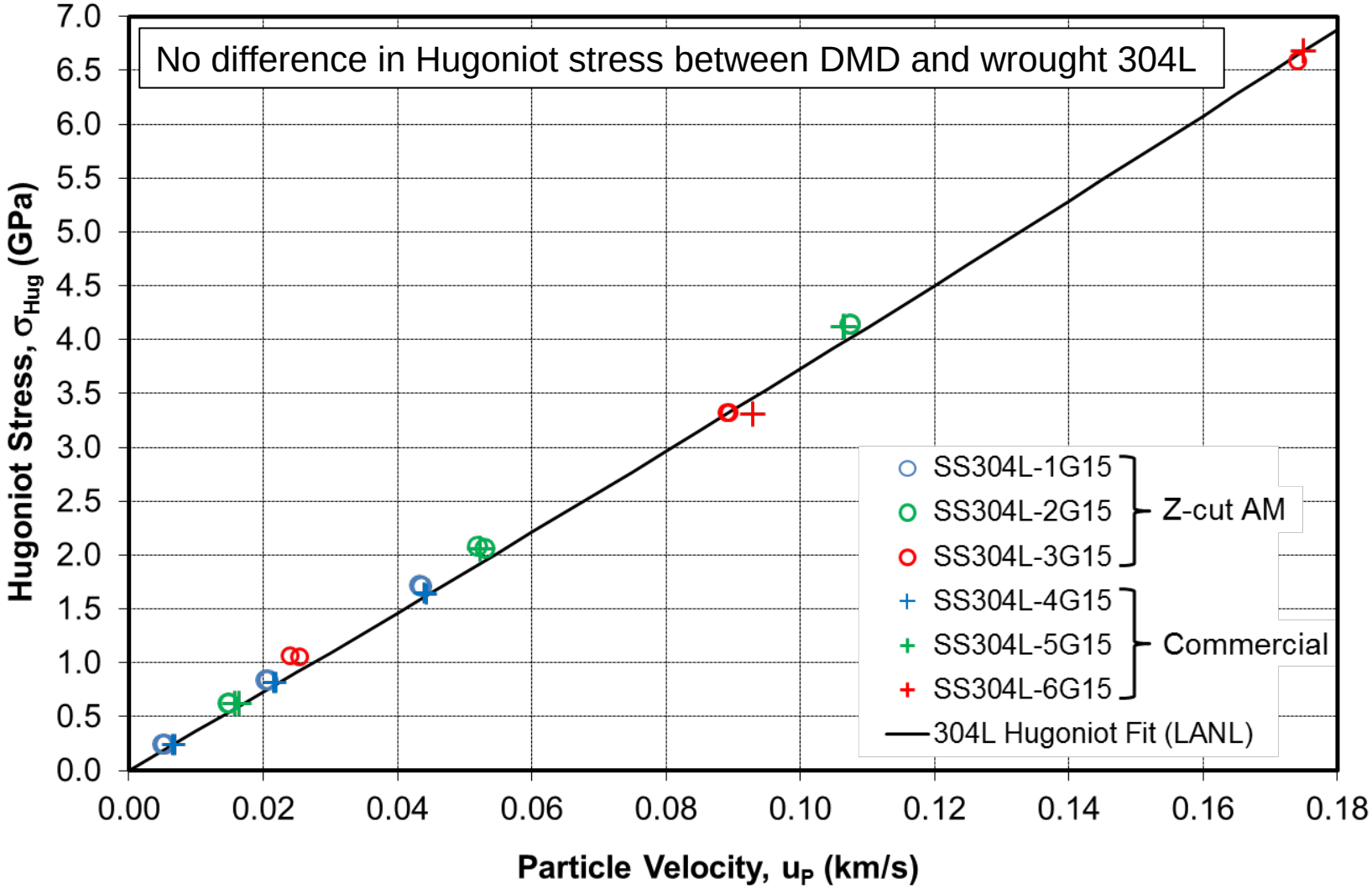

Spall Tests: Spall strengths of AM steel significantly exceed that of wrought.

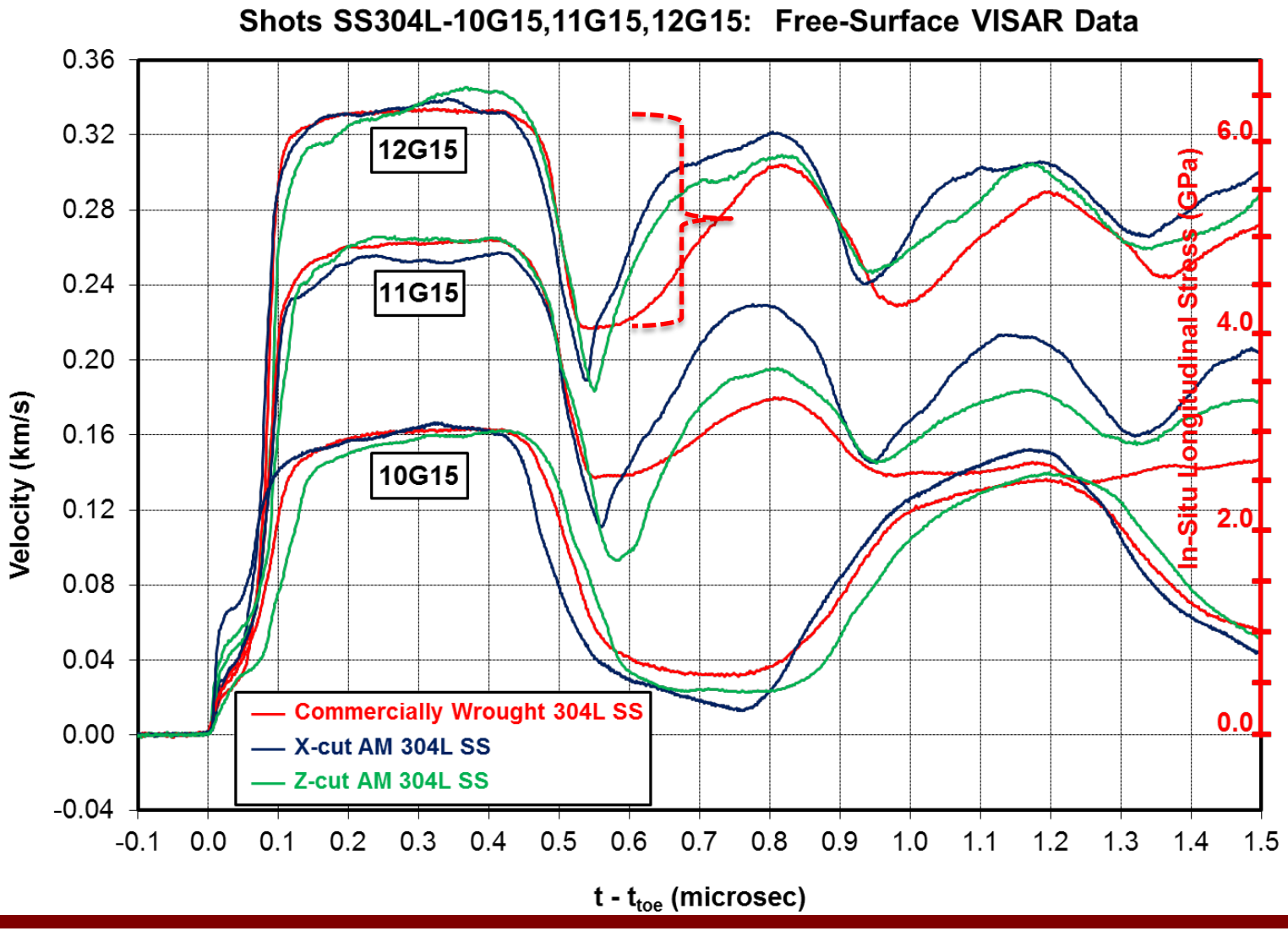

Mechanical Testing Summary

- ***Quasi-static testing (3.8 kW, 2.0 kW DED stainless steel 304L):***
  - Increased yield strength in AM compared to wrought
  - Decrease in ductility in AM compared to wrought
  - Loading parallel with uniform parallel hatch directions shows the least variability in ductility
  - Testing normal to uniform parallel hatch directions shows greater variability in ductility
- ***Dynamic testing (3.8 kW, 2.0 kW DED stainless steel 304L):***
  - Smaller increases in yield strength in DED when compare to static results
  - Differences in yield strength between wrought and DED become less pronounced at higher strain rates
- ***Reverse-ballistic testing (3.8 kW AM stainless steel 304L):***
  - Hugoniot EOS data for Z-cut AM samples closely matches current and archival LANL results for conventionally wrought 304L stainless steel.
- ***Forward-ballistic testing (3.8 kW AM stainless steel 304L):***
  - Hugoniot Elastic Limit (HEL) for X-cut and Z-cut AM material exhibits test-to-test/sample-to-sample variability, ranging from ~0.5 to 1.2 GPa, compared to a value of ~0.4 to 0.5 GPa for the conventional material.
  - Spall strength of X-cut (3.27 – 3.36 GPa) and Z-cut (3.71 – 3.91 GPa) AM material significantly exceeds that of conventional material (2.63 – 2.88 GPa).

Mechanical properties of DED 304L are different than wrought (stronger, less ductile)… why?

- Dislocation substructure
- Solidification subgrain structure
- Solid solution strengthening (nitrogen)
- 2nd Phase Dispersion (ferrite)
- Grain boundary strengthening (e.g. Hall-Petch)
- Transformation strengthening (α')
- Texture effects

Running tally going forward to indicate possible effect or eliminate effect

Dislocation Substructure	Solidification Substructure	Solid Solution	2nd Phase	Grain Boundary	α' Transformation	Texture

Microstructure of Different 304L Forms

Sandia National Laboratories

	Wrought	AM, 3.8 kW	AM, 2.0 kW
Longitudinal	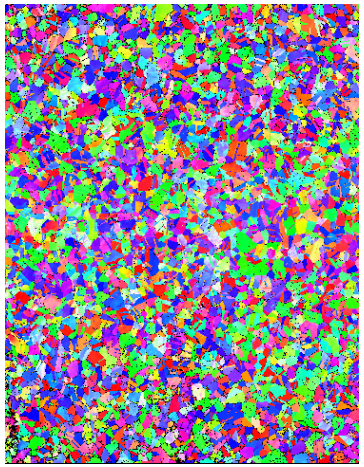		
Transverse	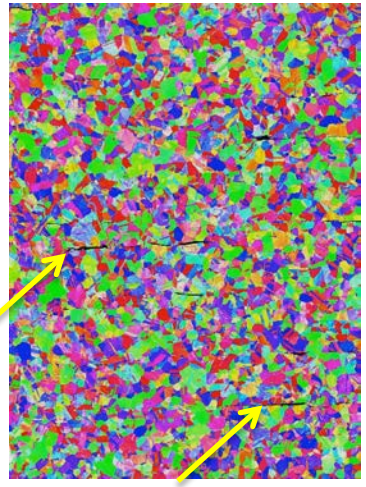		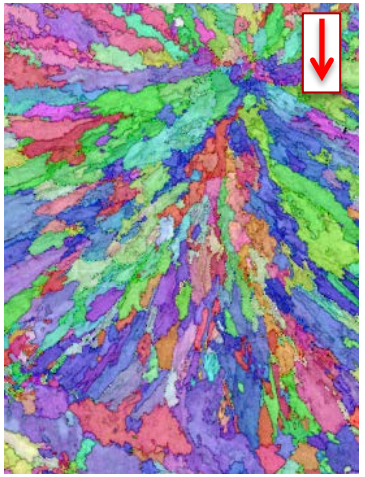

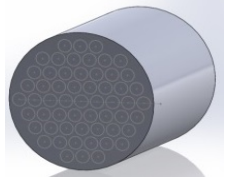

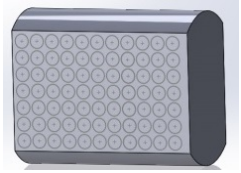

Ferrite stringers

1.0 mm

Dislocation Substructure | Solidification Substructure | Solid Solution | 2nd Phase | ~~Grain Boundary~~ | α′ Transformation | Texture

Anisotropy In Elastic Modulus

Material	Direction	Density (kg/m^3)	Shearmod (GPa)	Poisson's Ratio	Elastic Modulus (GPa)
Wrought B	X (axial)	7854.5	77.8	0.29	201.3
Wrought B	Y (trans)		77.6	0.29	200.5
Wrought B	Z (trans)		77.8	0.29	201.0
3.8 kW X//	X	7842.9	86.6	0.24	215.5
3.8 kW X//	Y		89.6	0.26	225.7
3.8 kW X//	Z		70.5	0.33	187.6
		99.85	% dense		

- **Measure density, ρ**
- **Ultrasound**
  - **Measure shear wave speed, C_s**
  - **Measure dilatational wave speed, C_d**
- **Zener anisotropy ratio = 3.78 (Ledbetter, 1984)**

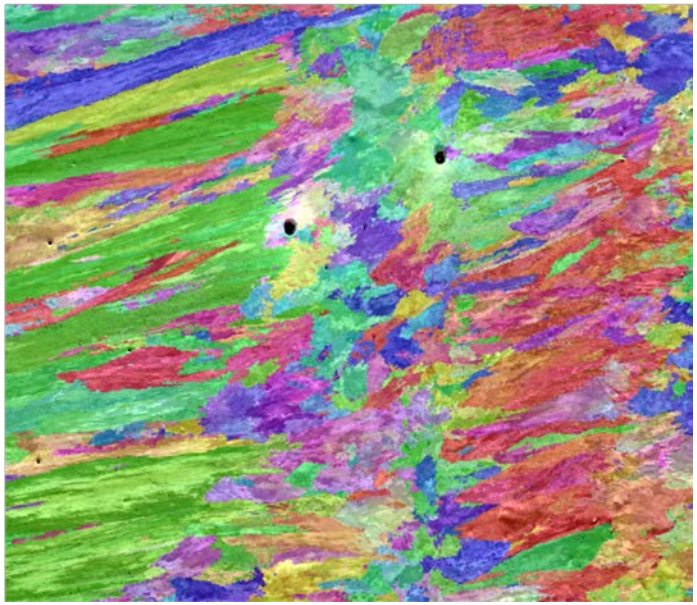

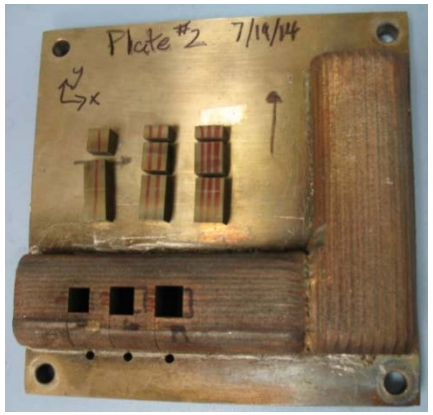

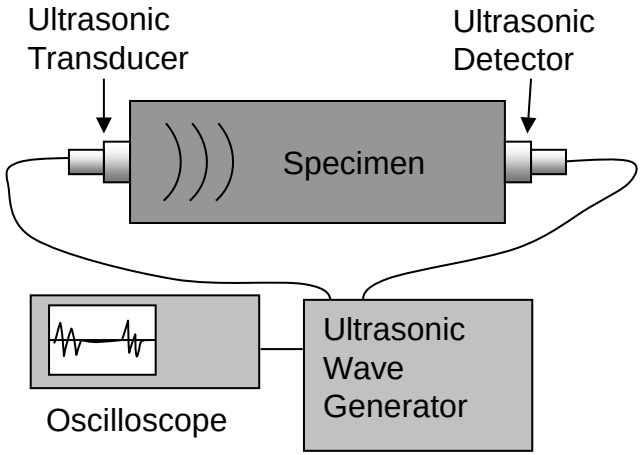

Dislocation Substructure | Solidification Substructure | Solid Solution | 2nd Phase | ~~Grain Boundary~~ | α′ Transformation | Texture

Anisotropy Predictions from Direct Numerical Simulation

EBSD texture data from the 3 orientations imprinted on Voronoi tesselated mesh

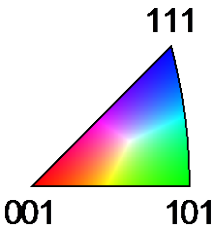

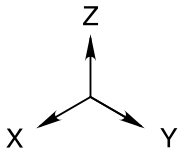

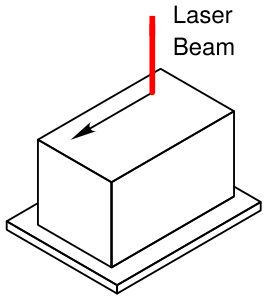

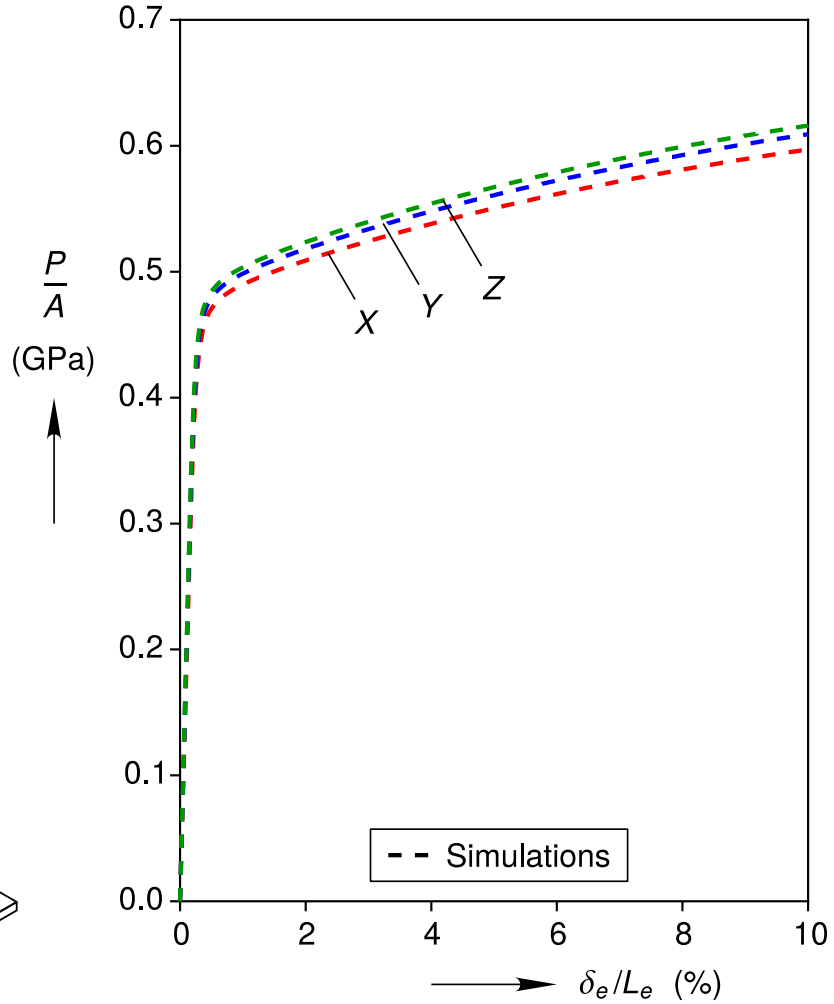

Dislocation Substructure | Solidification Substructure | Solid Solution | 2nd Phase | ~~Grain Boundary~~ | α′ Transformation | ~~Texture~~

Variation in Hardness Along Height

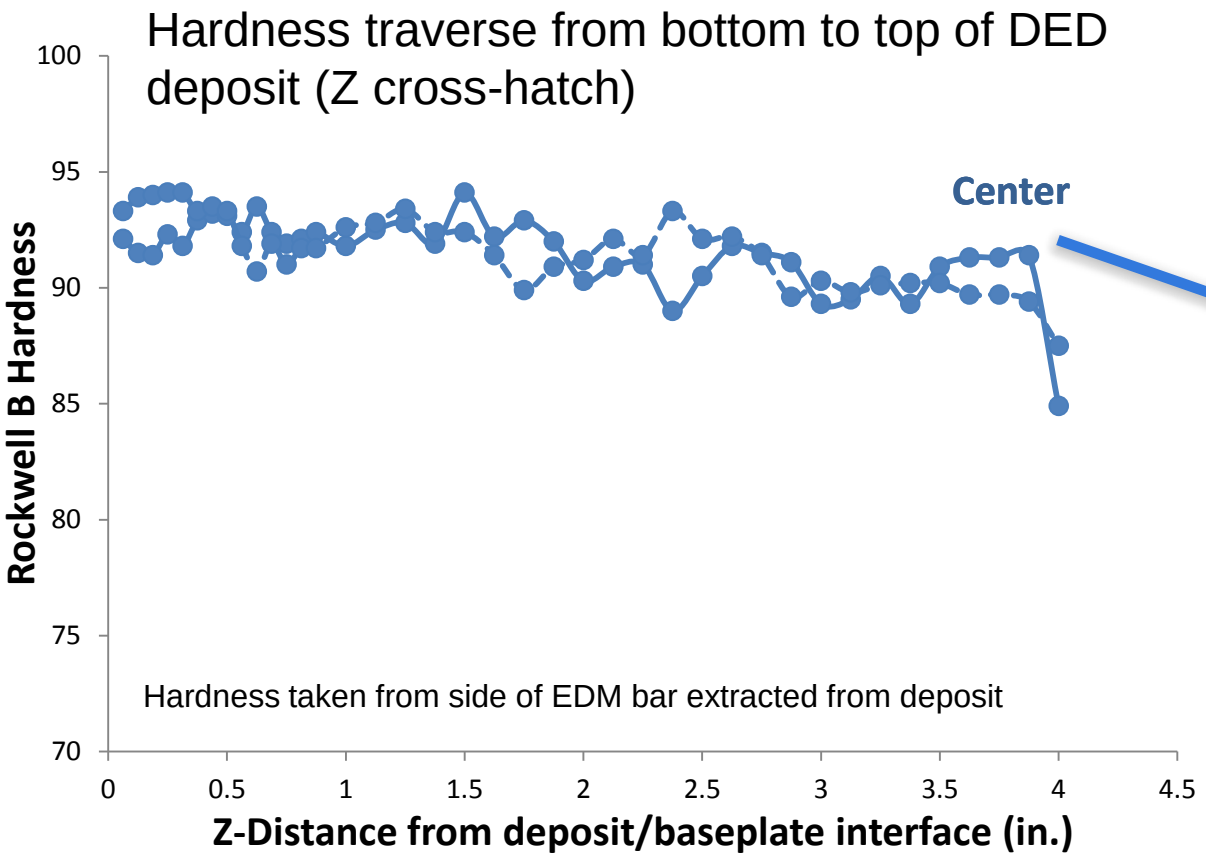

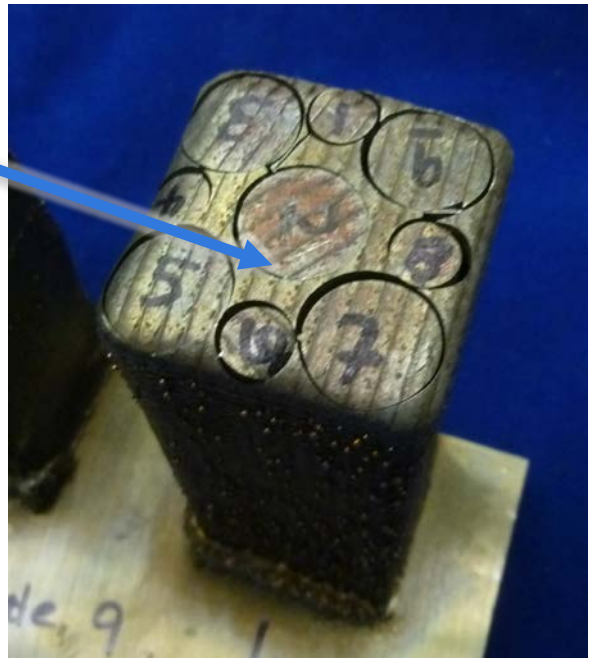

Dislocation Substructure	Solidification Substructure	Solid Solution	2nd Phase	~~Grain Boundary~~	α′ Transformation	~~Texture~~

Variation in Hardness Along Height and Position

Positional variation indicates that residual stress state may be playing a role, although some relaxation as the samples are extracted and machined is unavoidable.

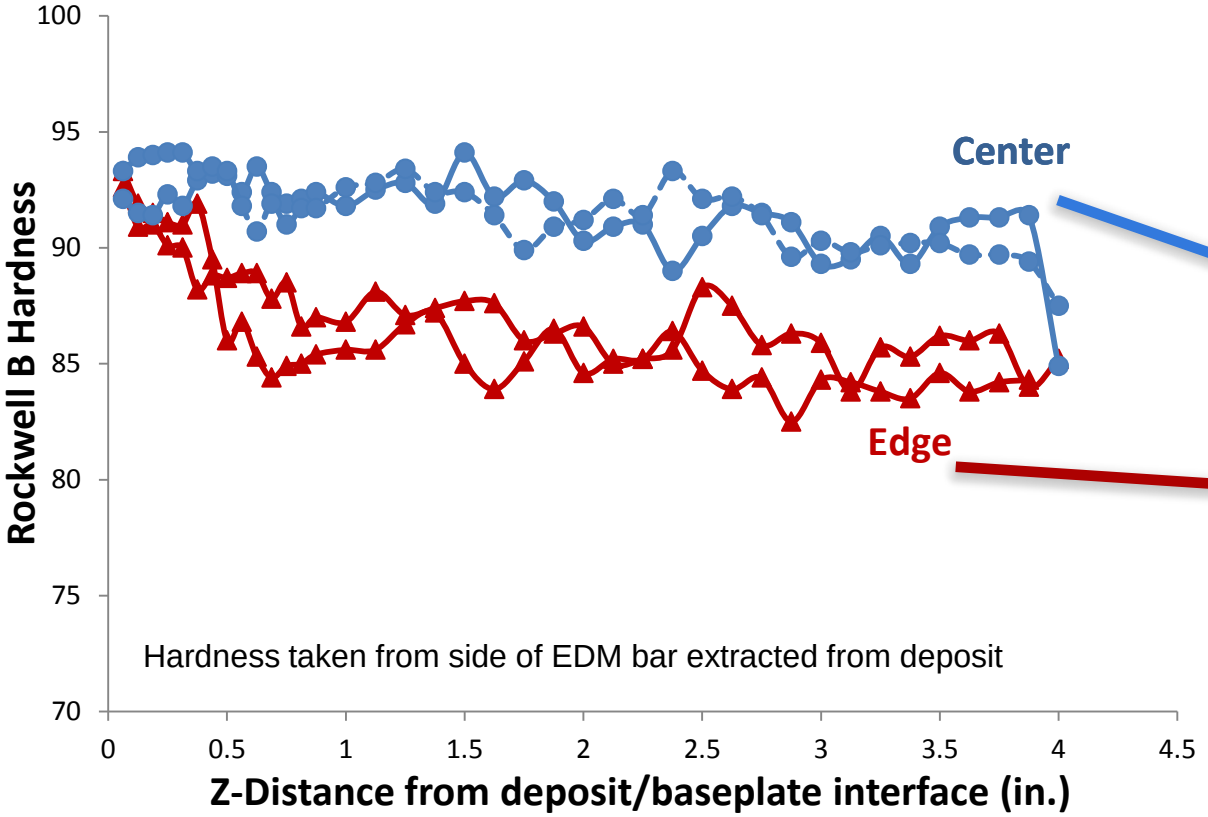

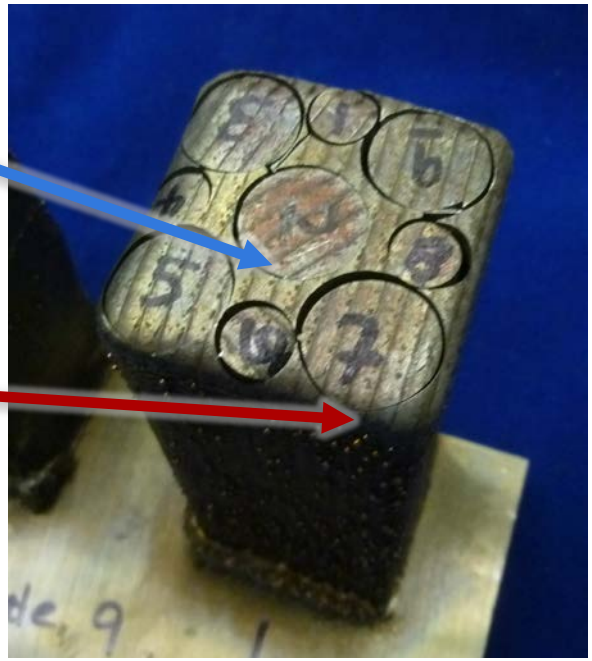

Hardness traverse from bottom to top of DED deposit (Z cross-hatch)

Variation in Hardness Along Height

"Recovery Anneal" at 750C, 1 hr nearly eliminated hardness difference between center and edge.

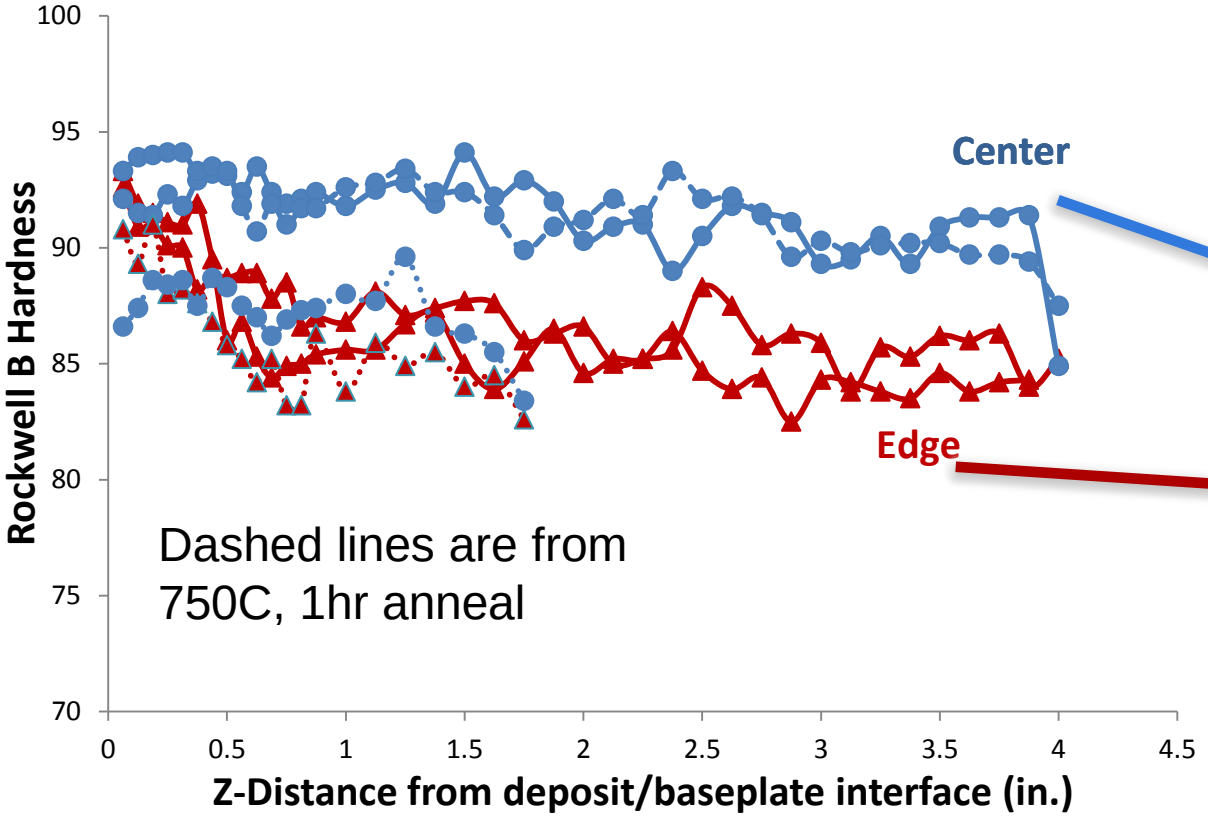

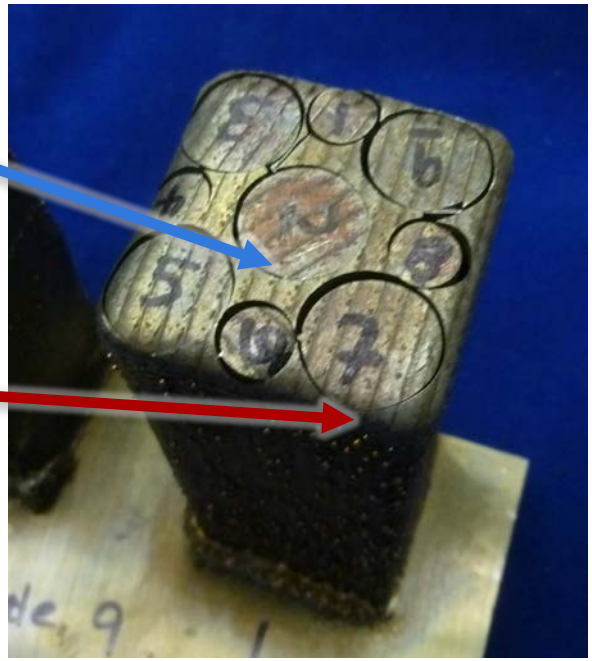

Dislocation Substructure	Solidification Substructure	Solid Solution	2nd Phase	~~Grain Boundary~~	α′ Transformation	~~Texture~~

After full annealing, DED deposit still harder than annealed wrought bar

Ferrite measurements from Ferritscope

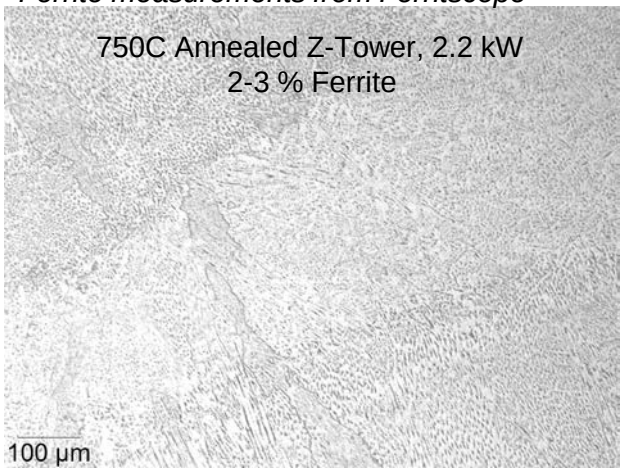

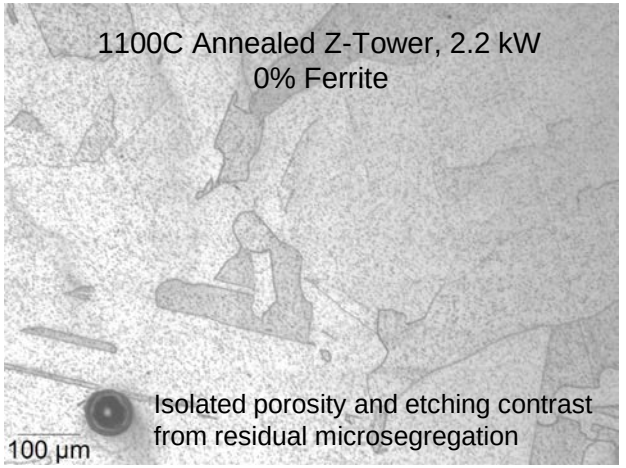

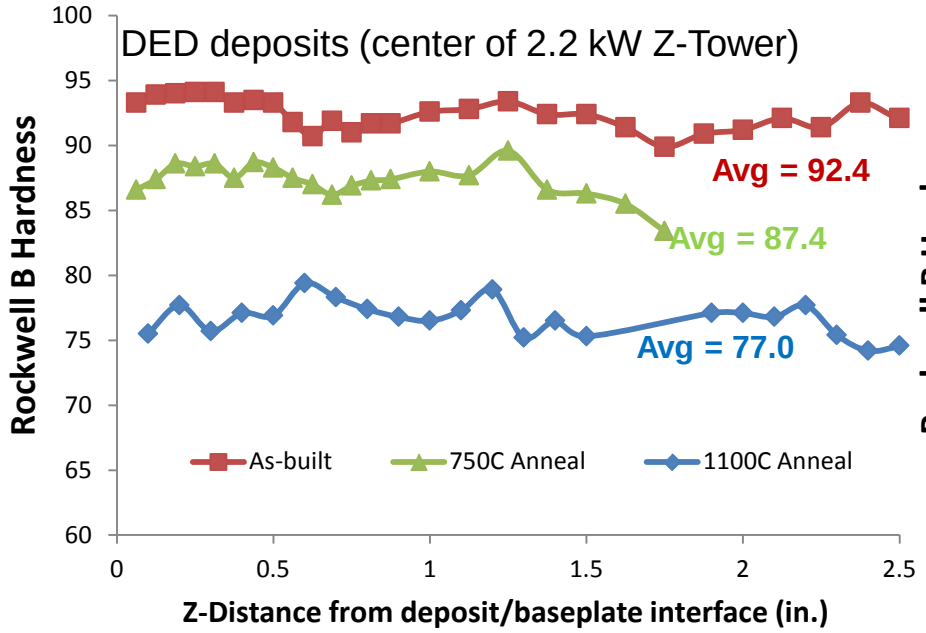

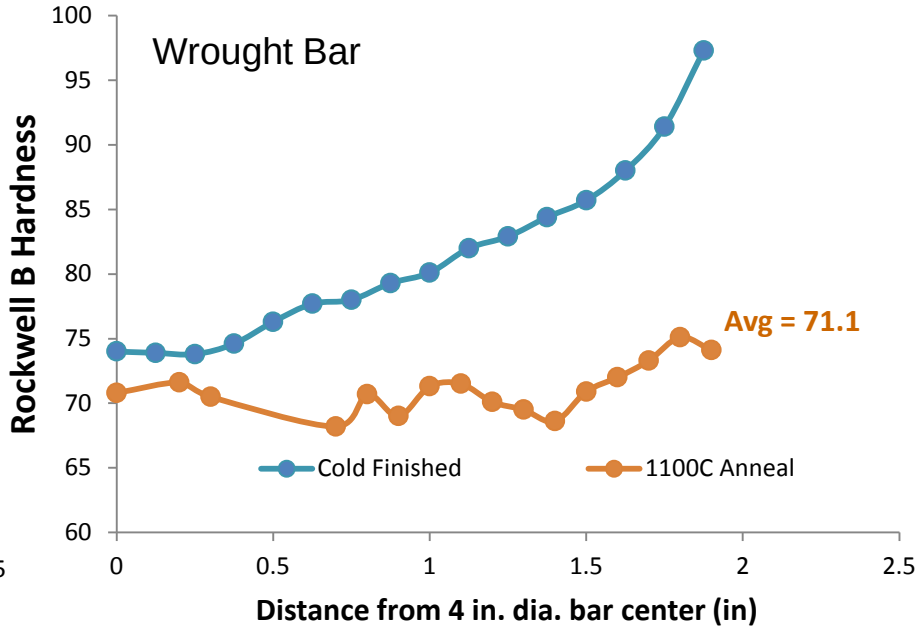

Dislocation Substructure	Solidification Substructure	Solid Solution	2nd Phase	~~Grain Boundary~~	α′ Transformation	~~Texture~~

Annealing Study

- 750C Annealing study could indicate effect of:
  - Grain and Subgrain Boundary Strengthening
  - Dispersion Strengthening of austenite from ferrite
  - Hard to isolate effect of each of these as they were eliminated with 1100C anneal
- 1100C Annealing study indicates effect of:
  - Likely only remaining effect is the result of nitrogen solid solution strengthening

	Cr	Ni	Mn	Si	Mo	Cu	N	P	C	S	O
Powder	19.07	10.38	1.55	0.50	0.04	0.03	**0.089**	0.009	0.013	0.006	0.017
Bar	19.5	10.1	1.5	0.58	0.027	ND	**0.049**	0.015	0.013	0.015	ND

Dislocation Substructure | Solidification Substructure | Solid Solution | 2nd Phase | ~~Grain Boundary~~ | α′ Transformation | ~~Texture~~

Solidification of 304L

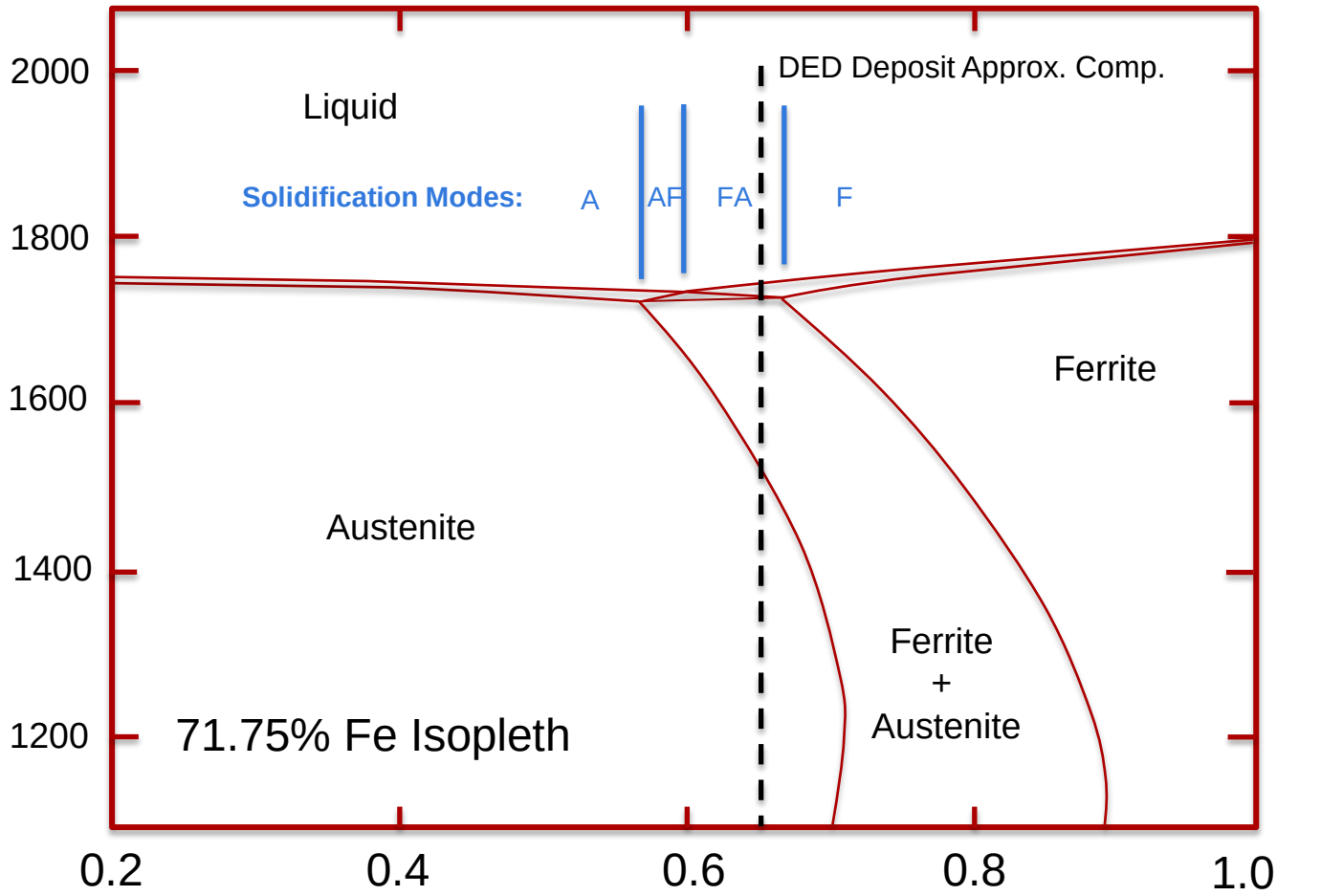

After Sorenson and Nelson, Proc. Of the 7th International Conf. on Trends in Welding Research, May 16-20, 2005, Pine Mtn. Georgia, 441-446

Dislocation Substructure	Solidification Substructure	Solid Solution	2nd Phase	~~Grain Boundary~~	α′ Transformation	~~Texture~~

Constitution Diagrams

Predictors of solidification mode and final microstructure in weld deposits (GTAW, SMAW)

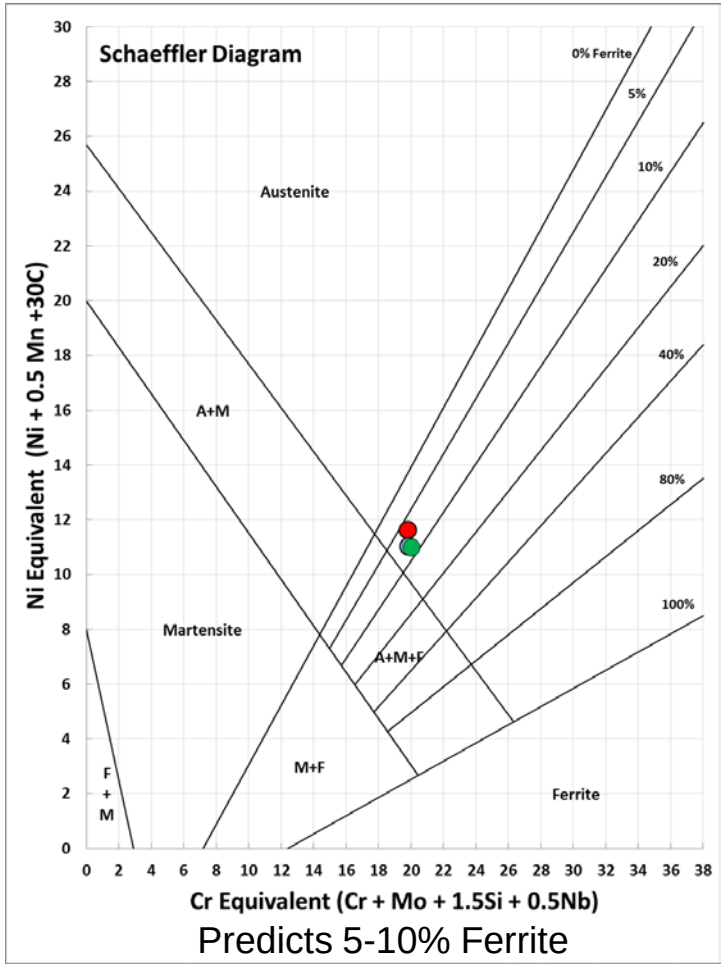

Predicts 5-10% Ferrite

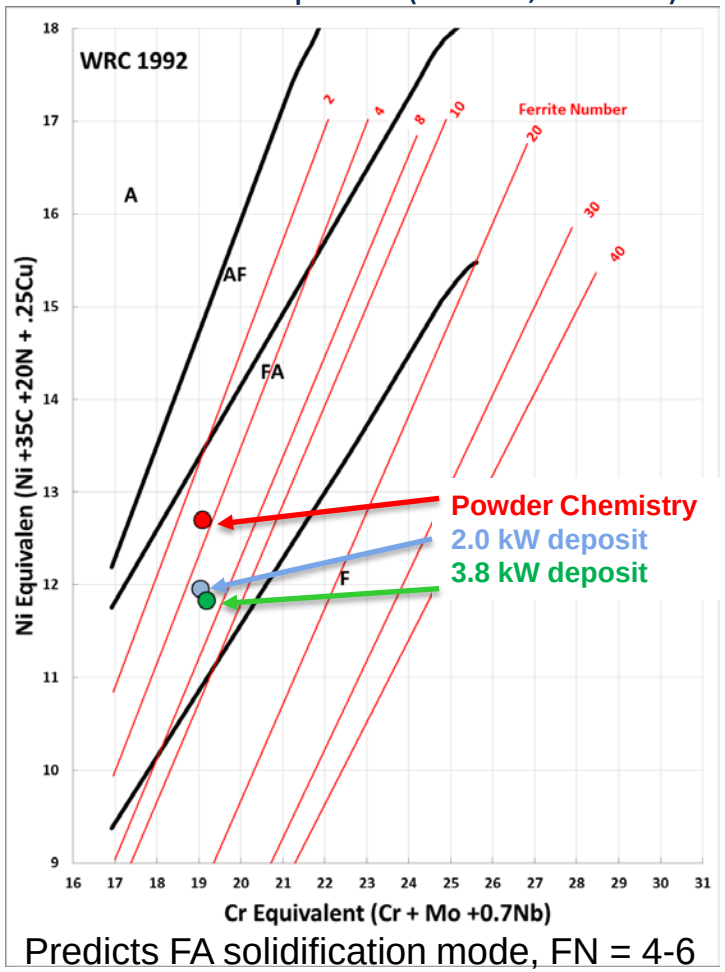

Predicts FA solidification mode, FN = 4-6

Constitution diagrams predict primary ferrite contents around 5-10%

Dislocation Substructure	Solidification Substructure	Solid Solution	2nd Phase	~~Grain Boundary~~	α′ Transformation	~~Texture~~

Primary Ferrite or Primary Austenite Solidification?

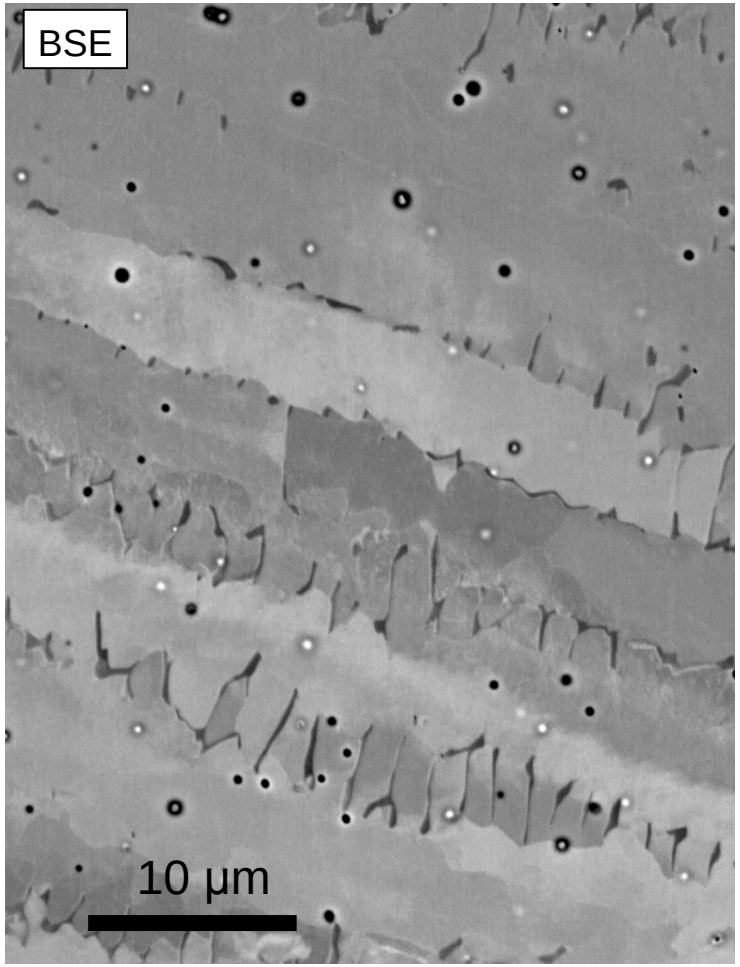

Dislocation Substructure | Solidification Substructure | Solid Solution | 2nd Phase | ~~Grain Boundary~~ | α′ Transformation | ~~Texture~~

304L DED (3.8 kW deposit)

Sandia National Laboratories

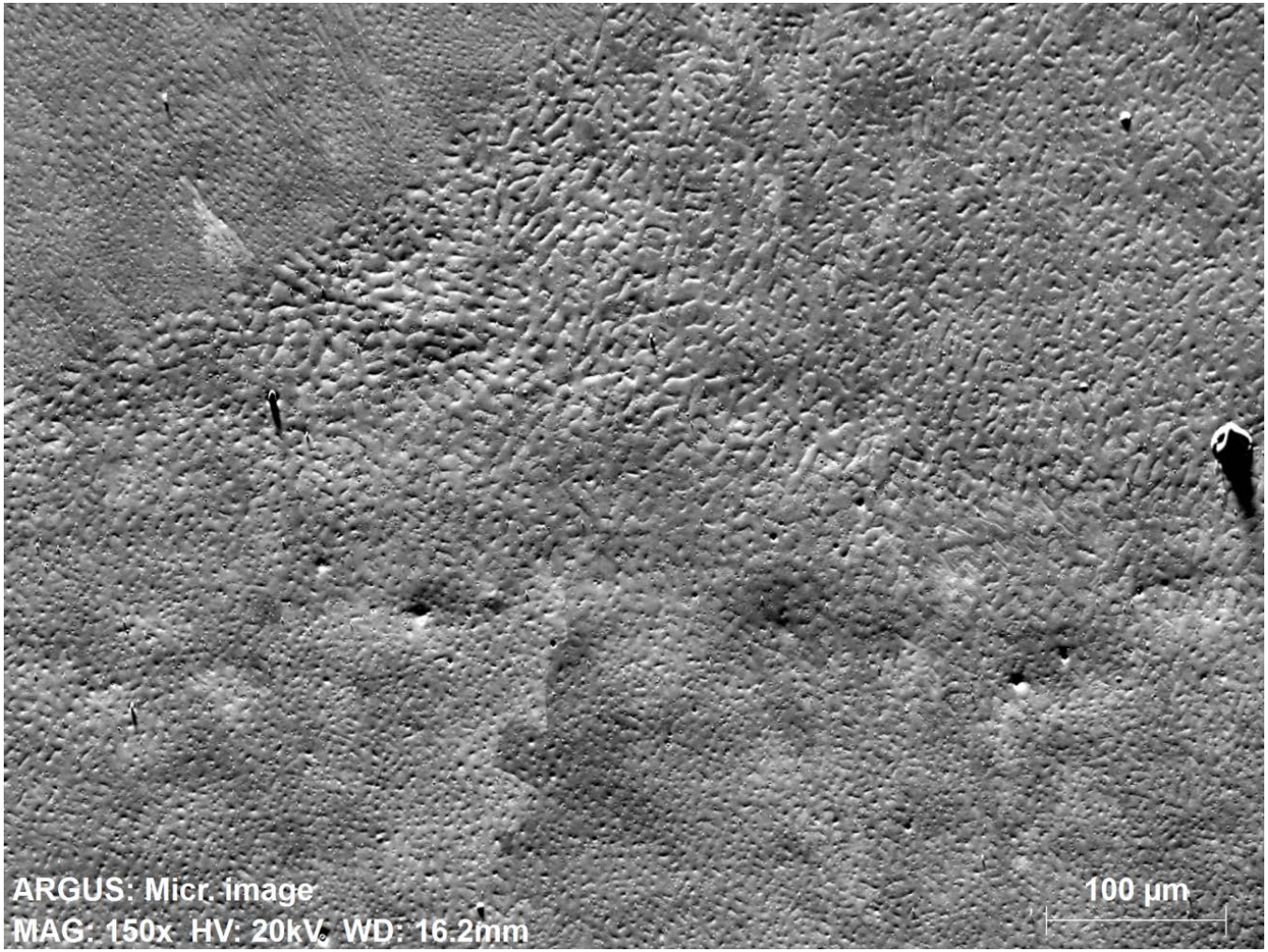

Forescatter electron image

Dislocation Substructure	Solidification Substructure	Solid Solution	2nd Phase	~~Grain Boundary~~	α′ Transformation	~~Texture~~

304L DED (3.8 kW deposit)

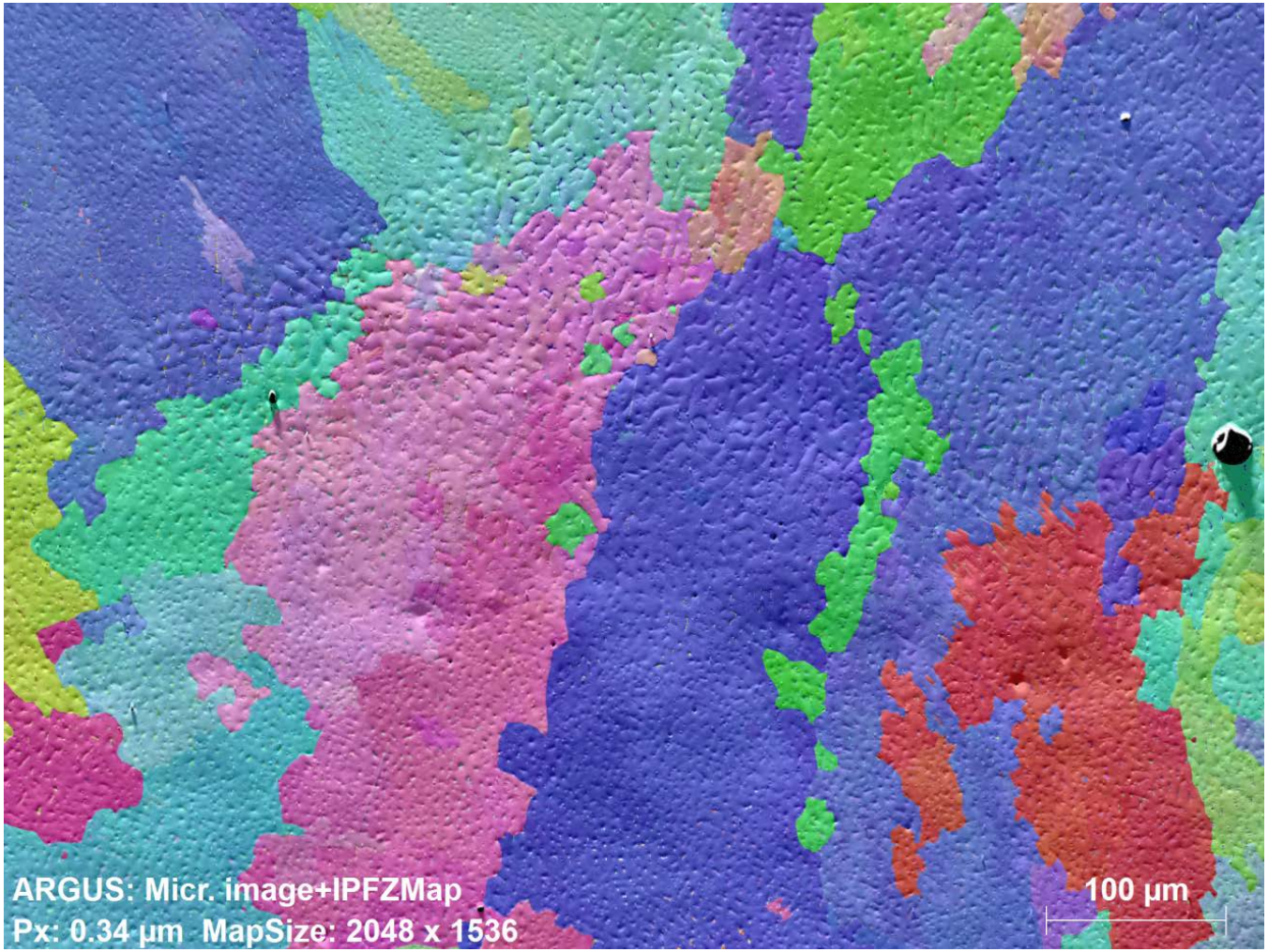

Image +EBSD Z IPF

Dislocation Substructure	Solidification Substructure	Solid Solution	2nd Phase	~~Grain Boundary~~	α′ Transformation	~~Texture~~

304L DED (3.8 kW deposit)

Sandia National Laboratories

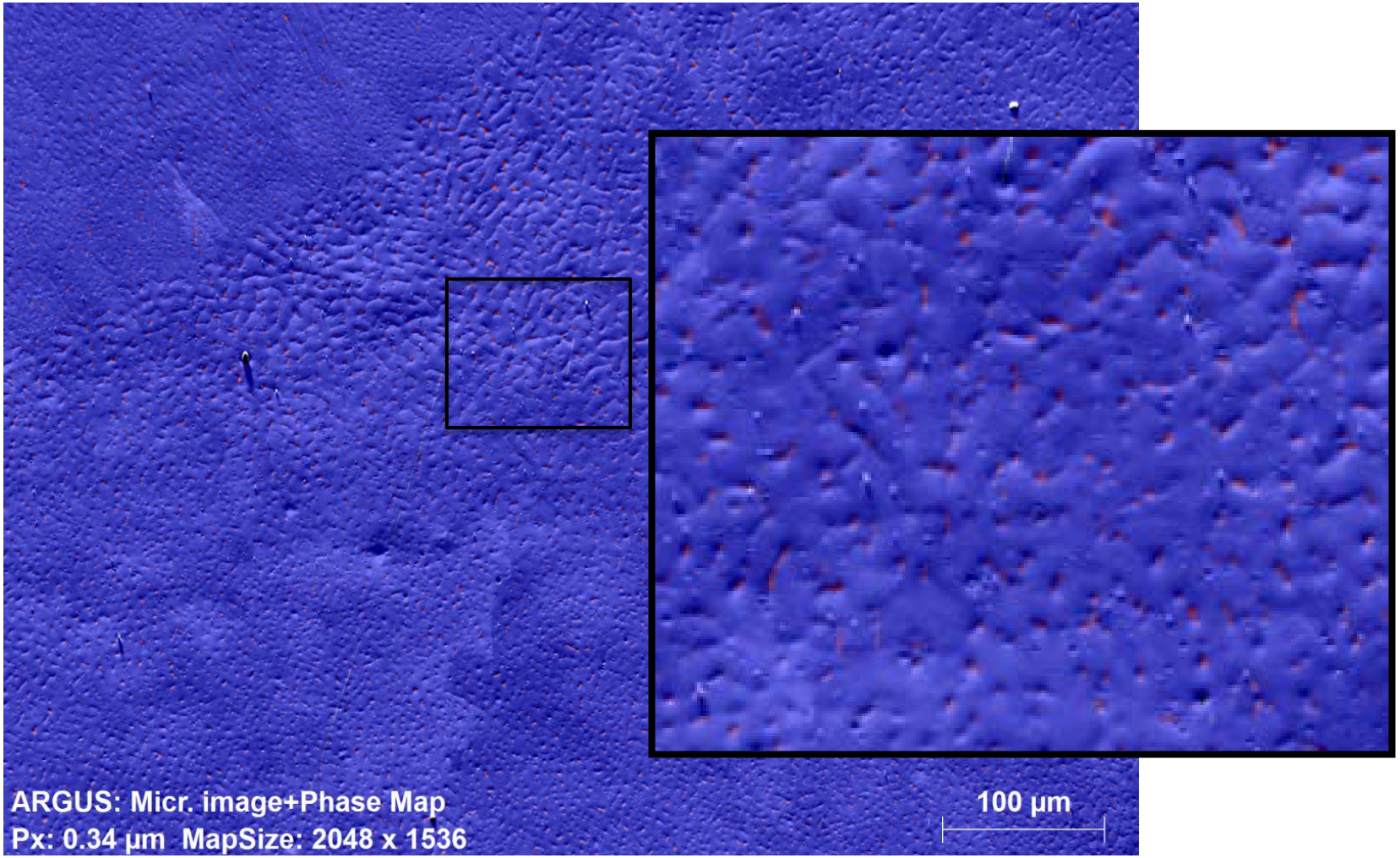

Image + austenite (blue)+ferrite (red)

Dislocation Substructure	Solidification Substructure	Solid Solution	2nd Phase	~~Grain Boundary~~	α′ Transformation	~~Texture~~

Primary Austenite or Primary Ferrite Solidification?

Sandia National Laboratories

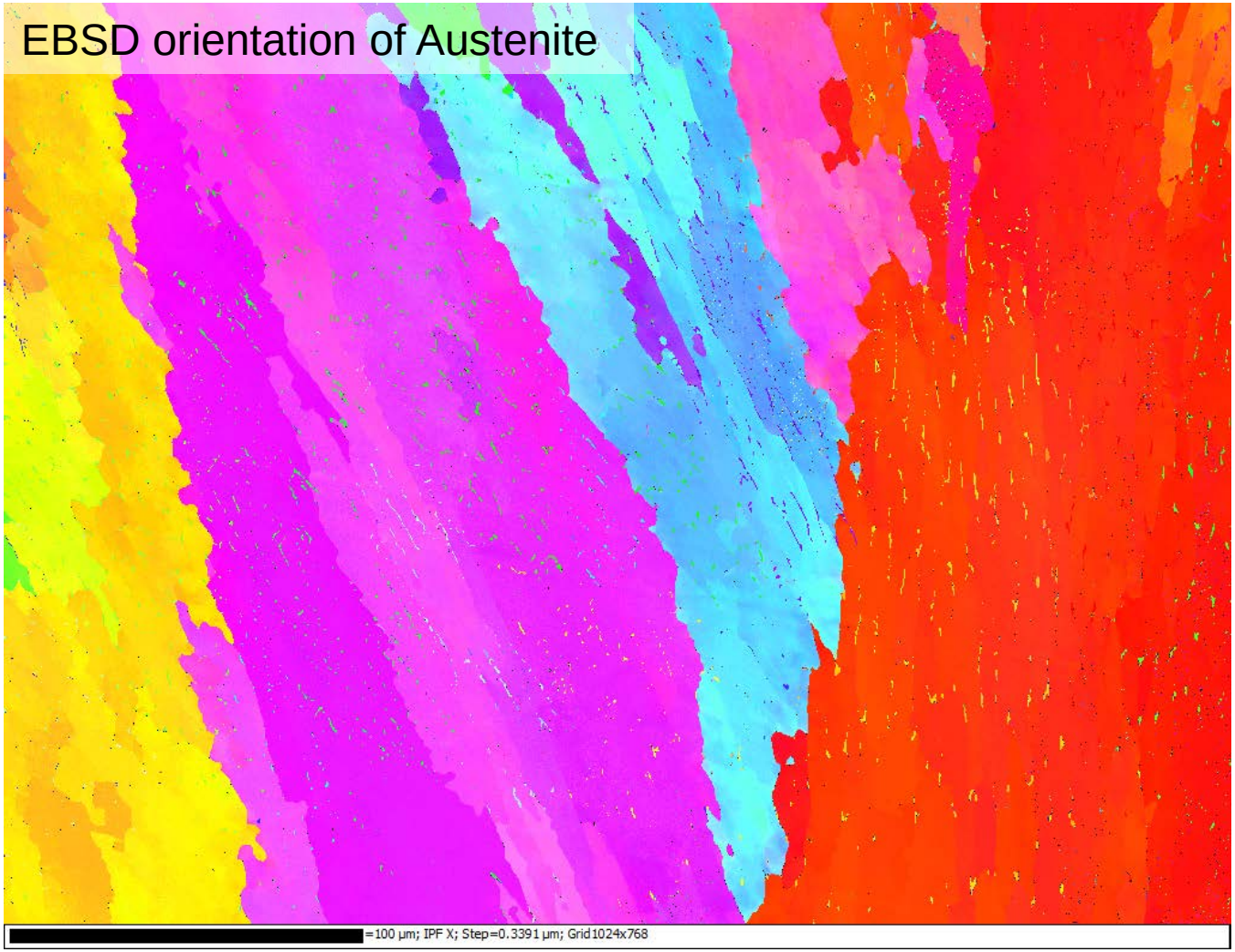

Dislocation Substructure | Solidification Substructure | Solid Solution | 2nd Phase | ~~Grain Boundary~~ | α′ Transformation | ~~Texture~~

Primary Austenite or Primary Ferrite Solidification?

Sandia National Laboratories

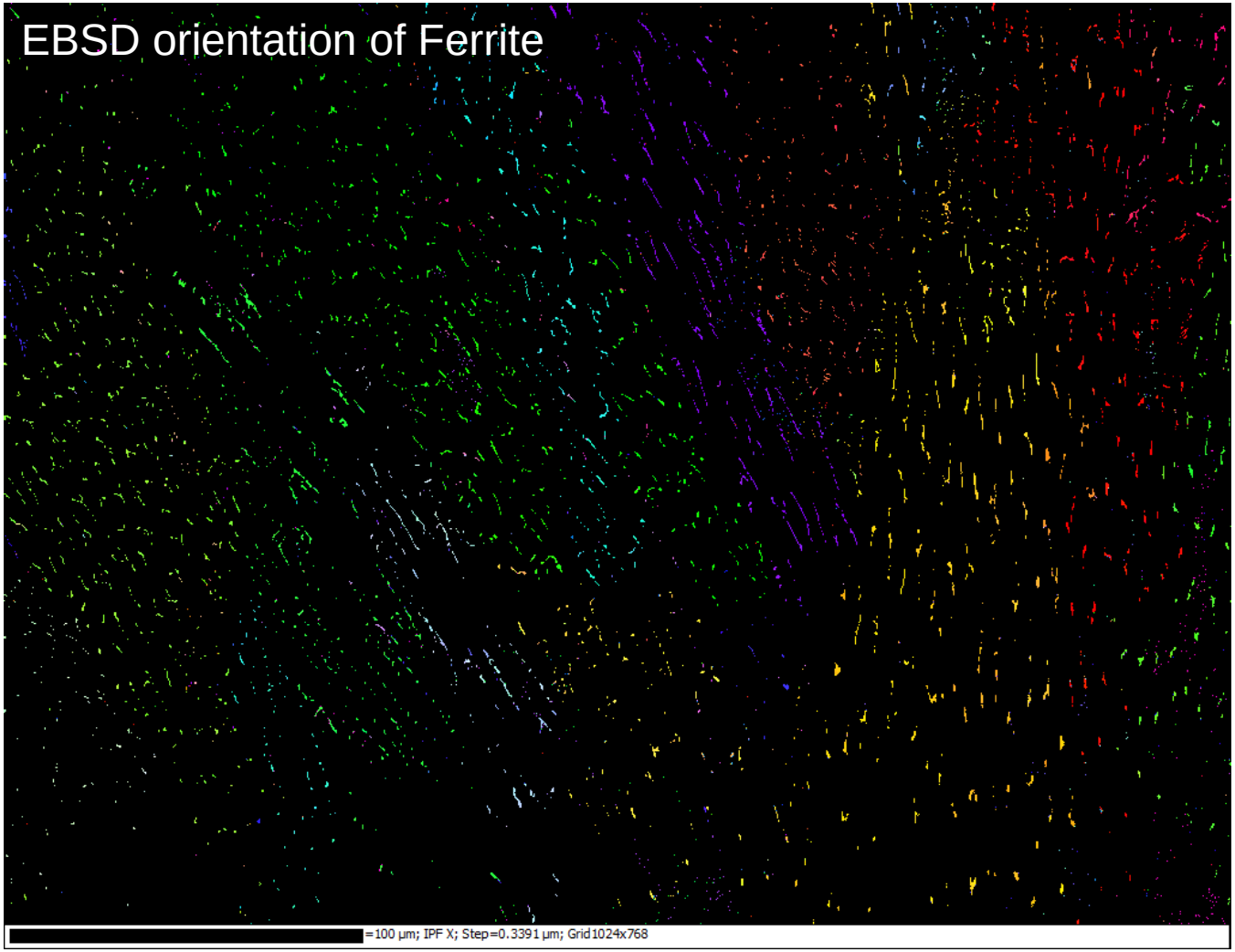

Dislocation Substructure	Solidification Substructure	Solid Solution	2nd Phase	~~Grain Boundary~~	α′ Transformation	~~Texture~~

Common Ferrite Orientation Within the Solidification Subgrains Indicative of Primary Ferrite Solidification

Sandia National Laboratories

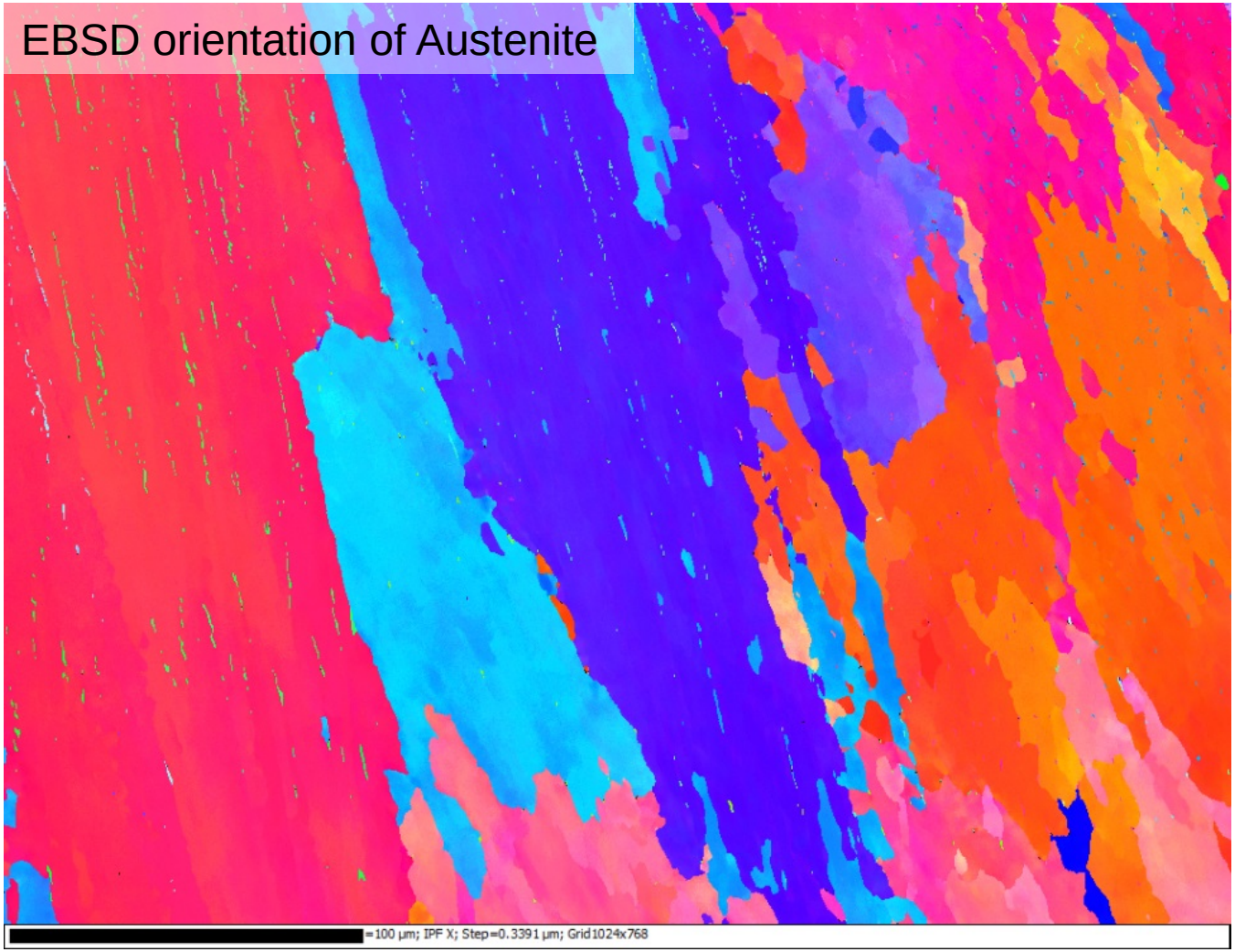

Dislocation Substructure | Solidification Substructure | Solid Solution | 2nd Phase | ~~Grain Boundary~~ | α′ Transformation | ~~Texture~~

Sandia National Laboratories

EBSD orientation of Ferrite

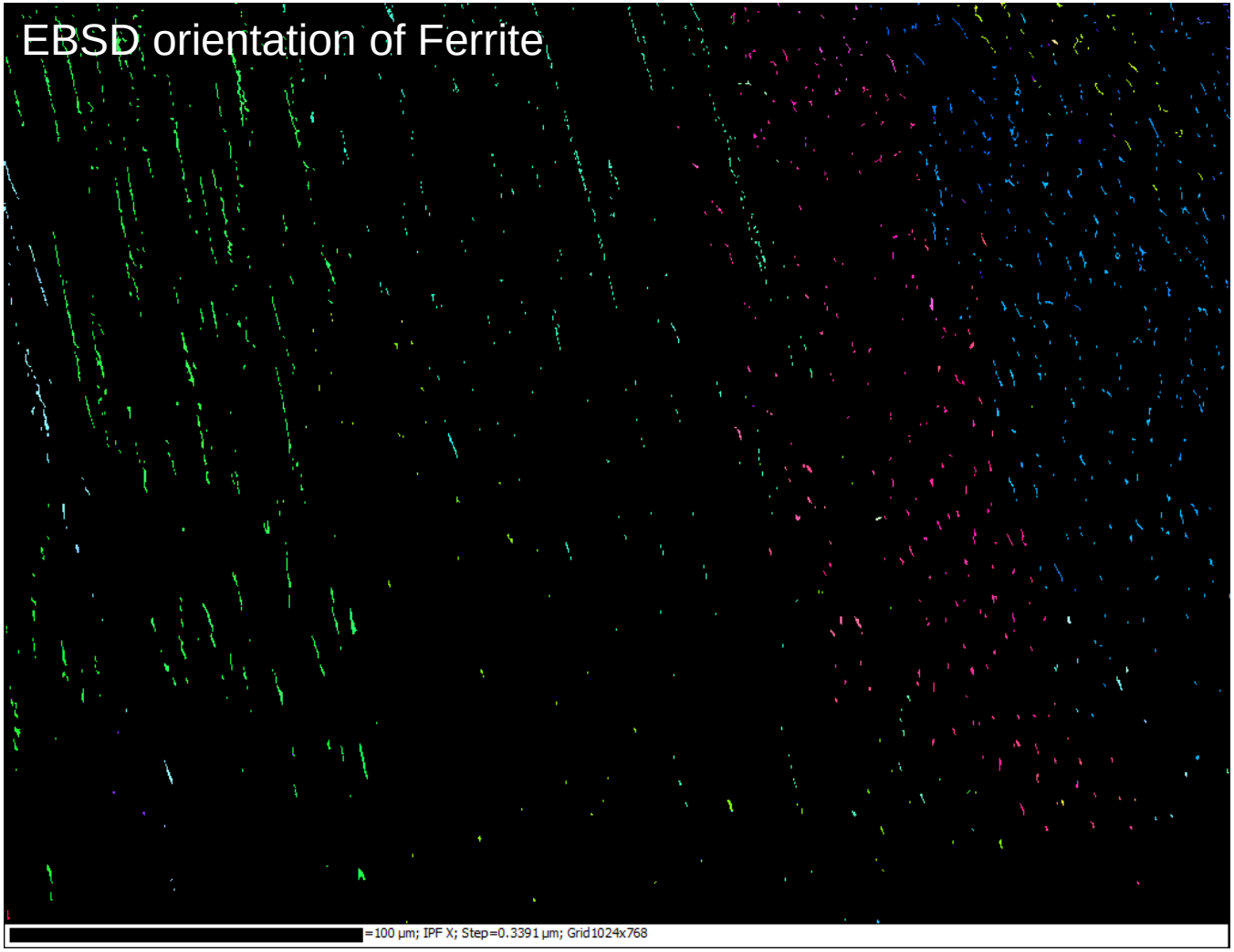

Dislocation Substructure | Solidification Substructure | Solid Solution | 2nd Phase | ~~Grain Boundary~~ | α′ Transformation | ~~Texture~~

Ferrite content has little effect on mechanical properties

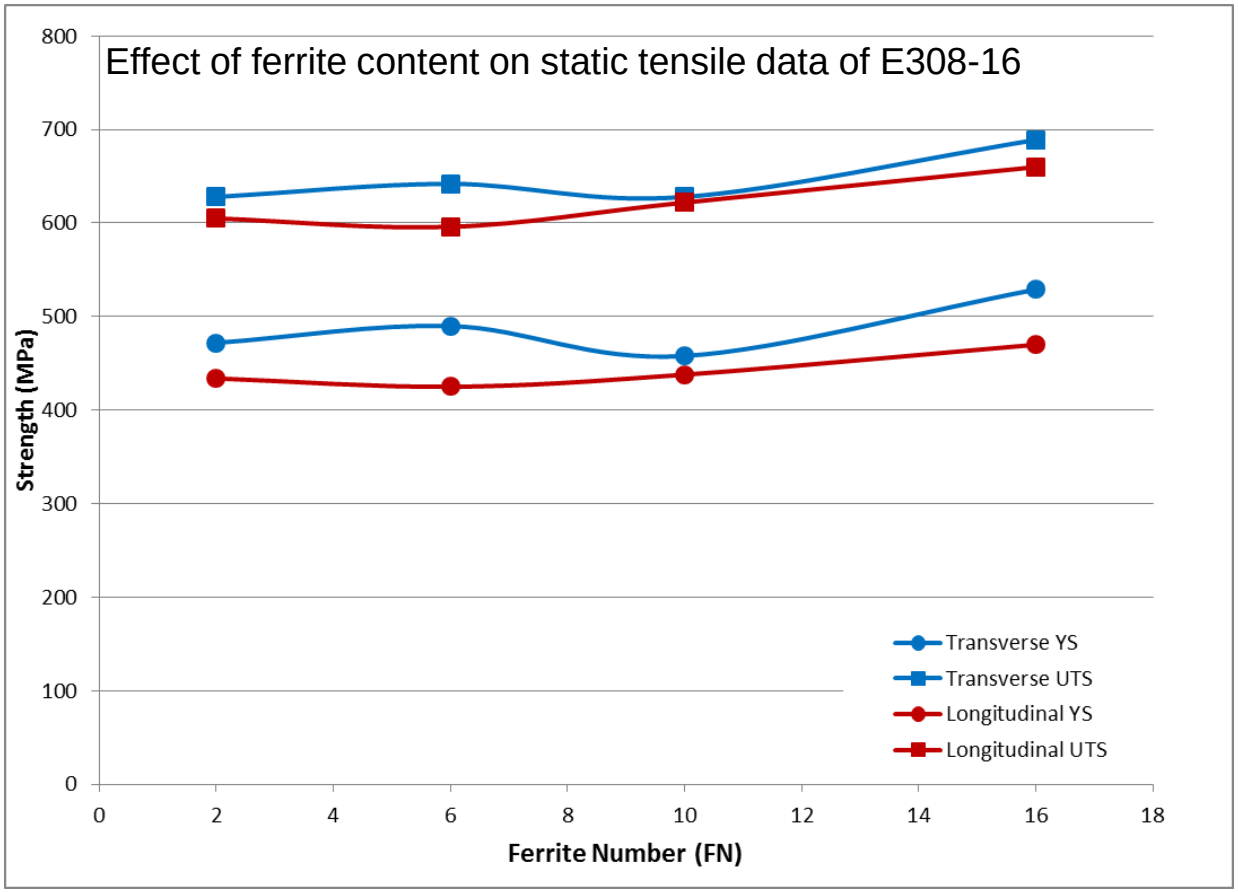

Reproduced from: D.Hauser and J.A. Vanecho, *Effects of Ferrite Content in Austenitic Stainless Steel Welds*, Welding Journal, Feb., 1982, 37s-44s.

Dislocation Substructure	Solidification Substructure	Solid Solution	~~2nd Phase~~	~~Grain Boundary~~	α′ Transformation	~~Texture~~

Neutron Diffraction at LANL is being used to quantify differences in dislocation density and how these change during deformation.

- Diffraction linewidth (FWHM) is increased with greater dislocation density (microstrain) and/or by decreased grain size.
- Initially greater dislocation density in AM material is consistent with observed FWHMs.
- With FWHM increasing during deformation, can expect dislocation density is represented within the diffracted beam width.

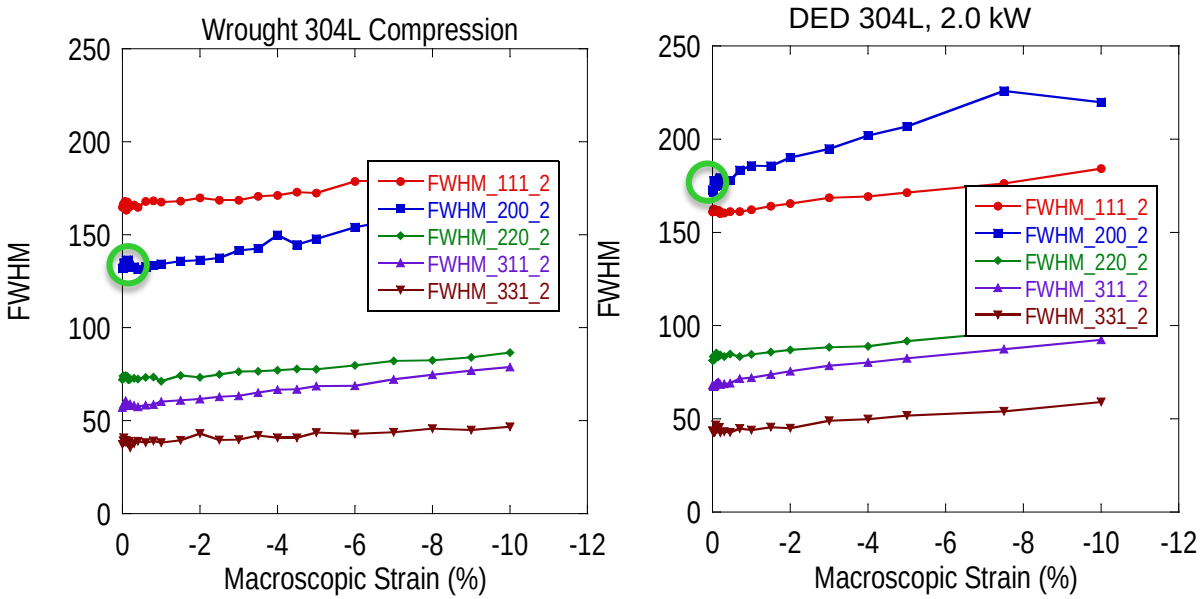

Data Courtesy: D. Brown, B.Clausen, J. Carpenter, LANL

Dislocation Substructure | Solidification Substructure | Solid Solution | ~~2nd Phase~~ | ~~Grain Boundary~~ | α′ Transformation | ~~Texture~~

Subgrain Structure (solidification subgrains)

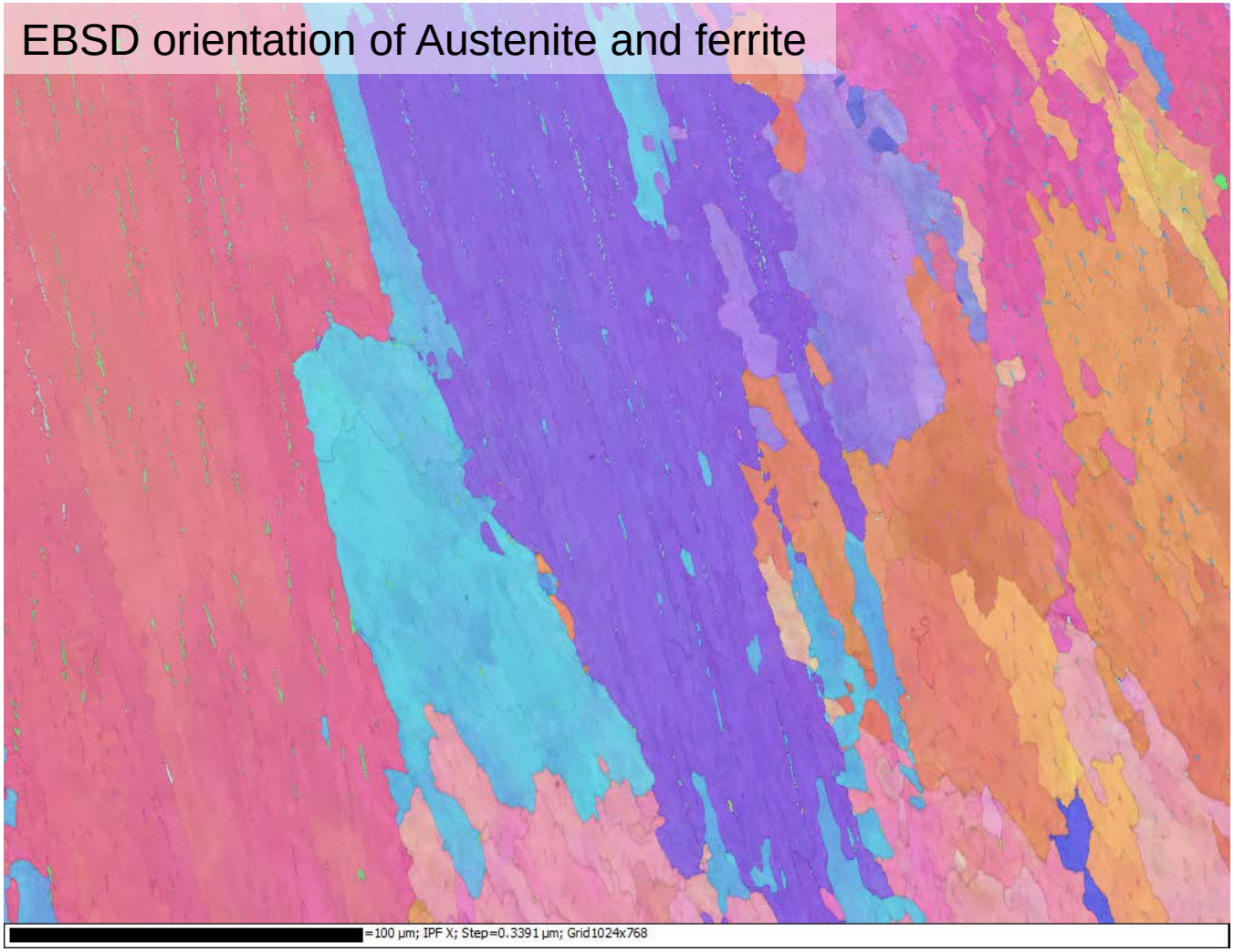

Dislocation Substructure | Solidification Substructure | Solid Solution | ~~2nd Phase~~ | ~~Grain Boundary~~ | α′ Transformation | ~~Texture~~

Subgrain Structure (solidification subgrains)

Sandia National Laboratories

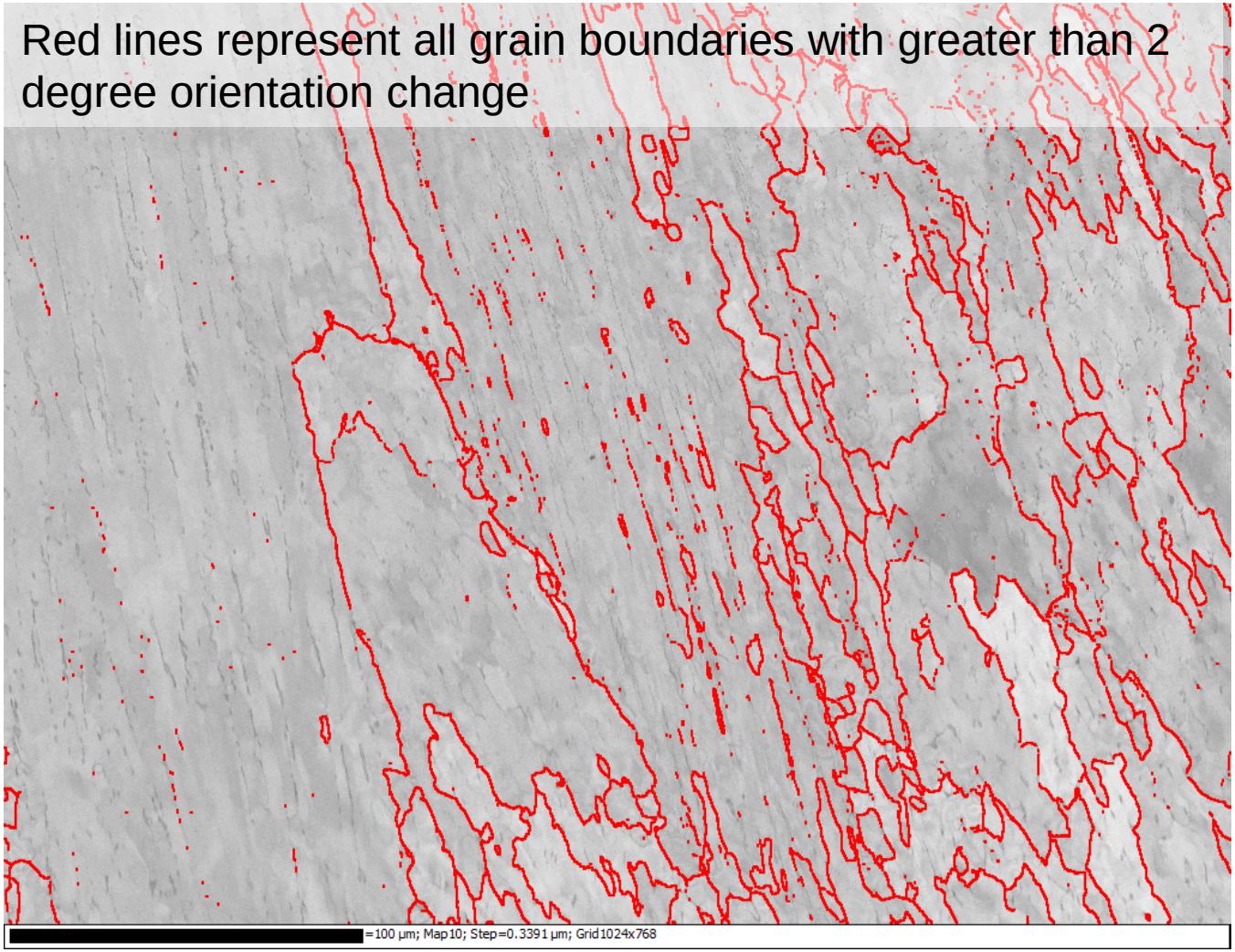

Dislocation Substructure | Solidification Substructure | Solid Solution | 2nd Phase | Grain Boundary | α′ Transformation | Texture

Misorientation between subgrains isnot enough to pose any significant barrier to dislocation motion

Sandia National Laboratories

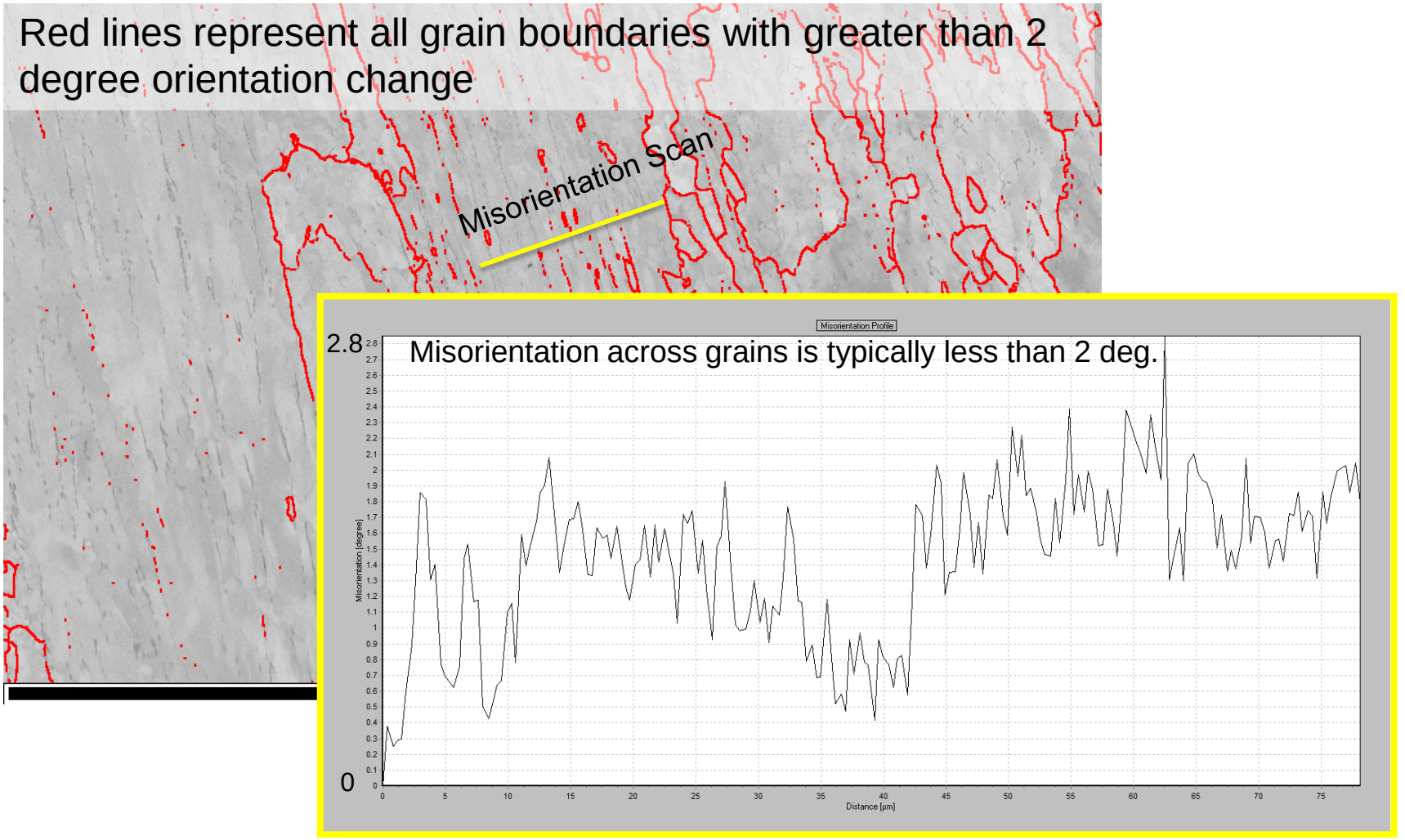

Dislocation Substructure | ~~Solidification Substructure~~ | Solid Solution | ~~2nd Phase~~ | ~~Grain Boundary~~ | α′ Transformation | ~~Texture~~

α' Transformation Tendency of Cored Microstructures

While DED material shows local variation in tendency to form martensite, the microstructure will likely form only slight amounts of martensite at room temperature

Sandia National Laboratories

(From high resolution WDS mapping of Ni, Cr, Mn, Mo, Si, C, N)

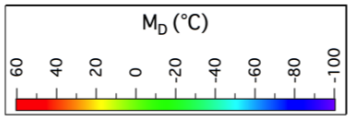

← Martensite **MORE** stable

Austenite **MORE** stable →

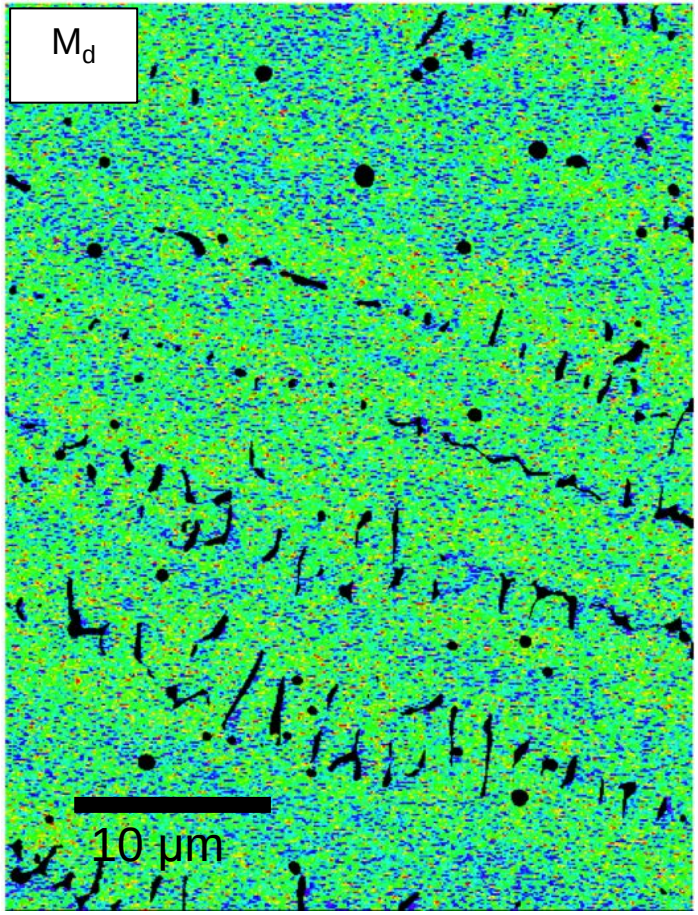

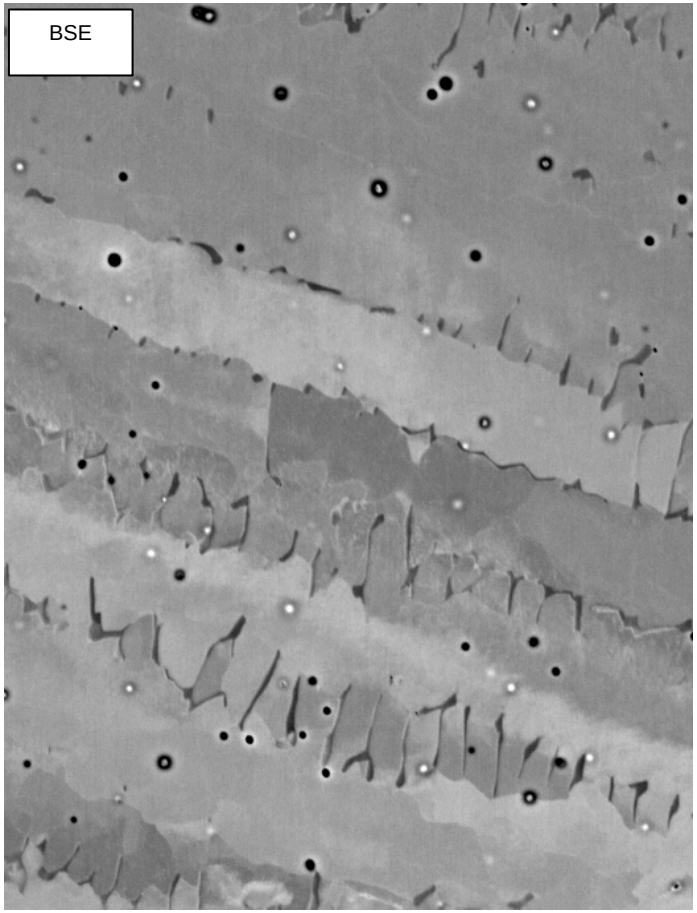

Angel et al. (1954)

M_d (ºC) = 413 – 13.7[Cr] – 9.5[Ni] -8.1[Mn] – 18.5[Mo] – 9.2[Si] – 462[C+N]

Dislocation Substructure	~~Solidification Substructure~~	Solid Solution	~~2nd Phase~~	~~Grain Boundary~~	α' Transformation	~~Texture~~

BCC content in LENS samples may increase slightly with tensile loading (Neutron Diffraction at LANL)

Volume transformed does not effect early yield stress

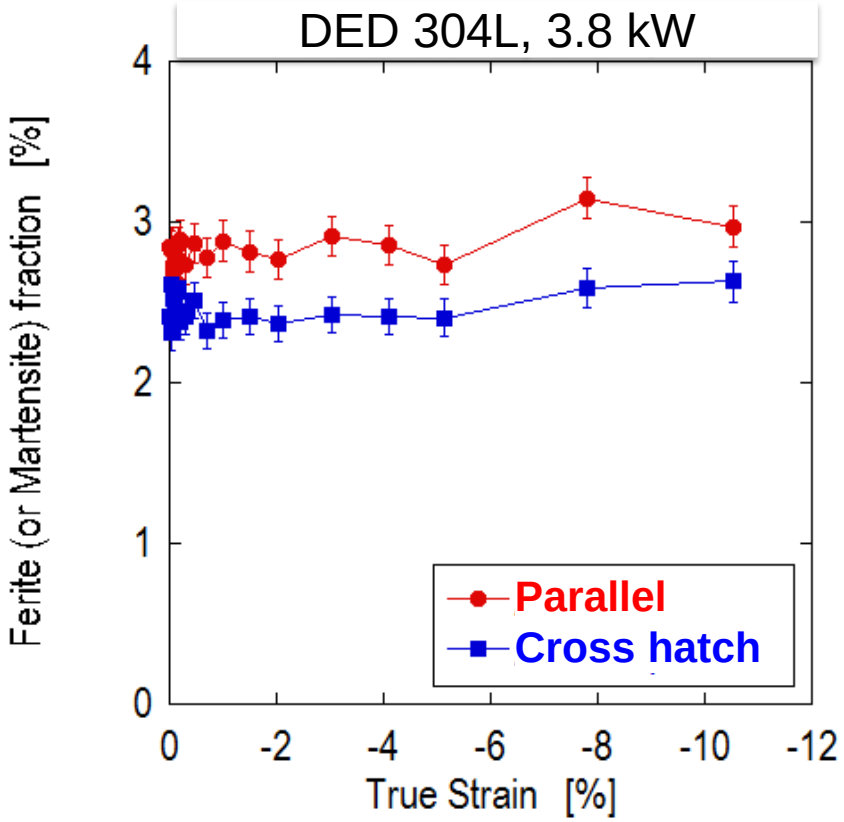

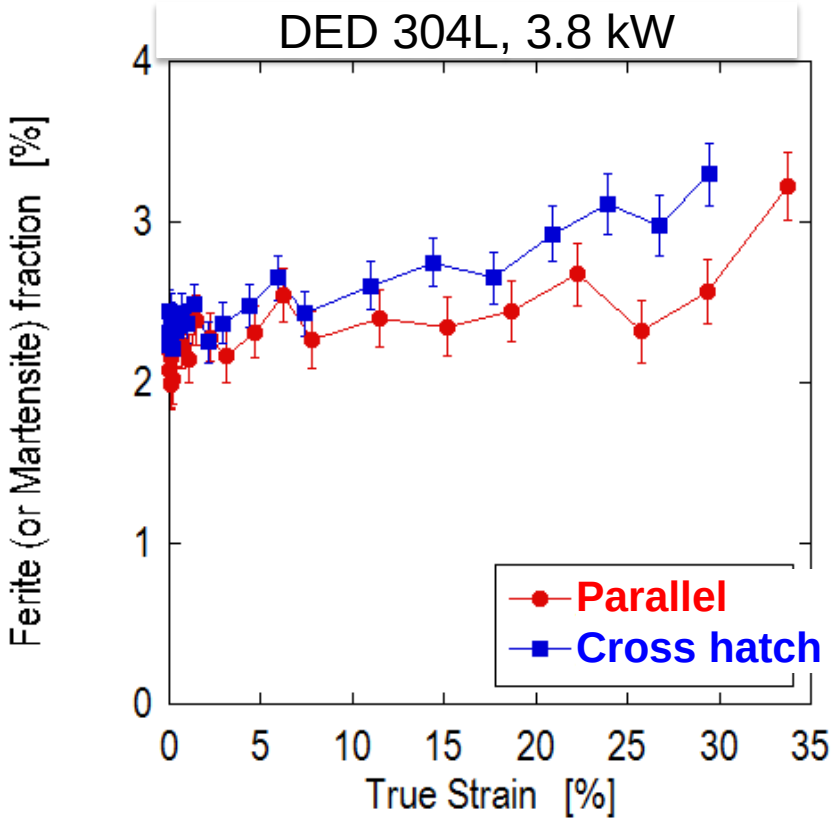

Data Courtesy: D. Brown, B.Clausen, J. Carpenter, LANL

Dislocation Substructure	Solidification Substructure	Solid Solution	2nd Phase	Grain Boundary	α′ Transformation	Texture

Summary (and what's next)

- Generally, DED 304L shows higher strength and lower ductility than its wrought counterpart
  - Dislocation substructure and solid solution strengthening (N) appear to be emerging as the main factors in increasing the strength of DED 304L
    - Teasing out the effect of these two will require more focused annealing studies, fine structure examination, and residual stress characterization
  - Build style (hatching orientation, power), test location and test orientation all contribute to the variability observed in the 304L deposits
    - Shear + torsion testing in process, and off-axis compression testing
  - Oxides, occasional porosity were observed
    - Oxides not prevalent enough to effect flow stress
    - Porosity, while not prevalent, can have more of an impact on ductility than flow stress
    - Fractography of low and high results to be pursued to assess defects that may have led to outlier positions

Acknowledgments

- LDRD Program Office
- LANL for neutron diffraction activities
- A.C. Kilgo, B.B. McKenzie, R. Grant for metallography, SEM and WDS
- Whoever Todd Palmer chained to the DMD unit to make us 200 lbs of 304L deposits

Summary of DED static tensile data

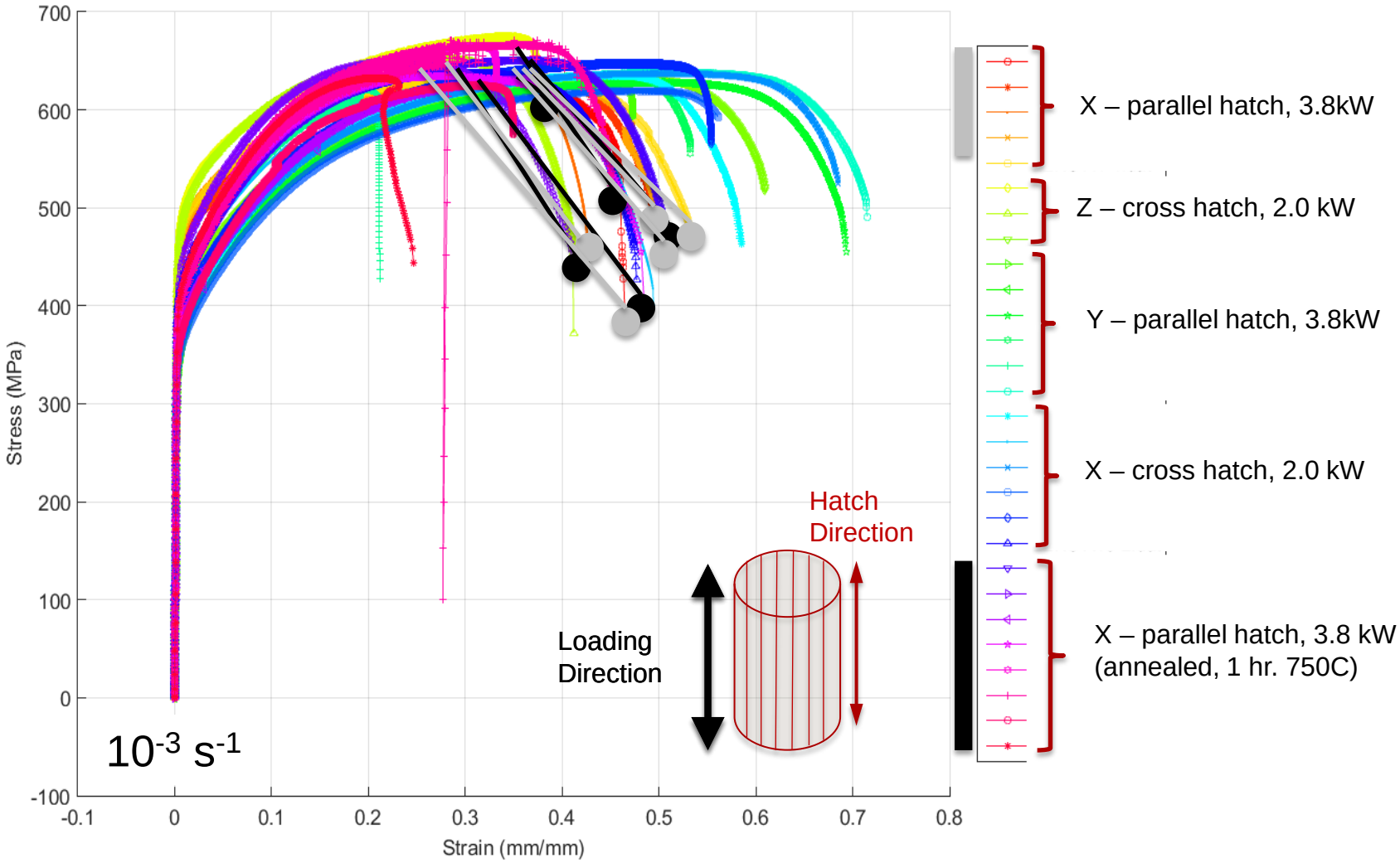

Summary of DED static tensile data

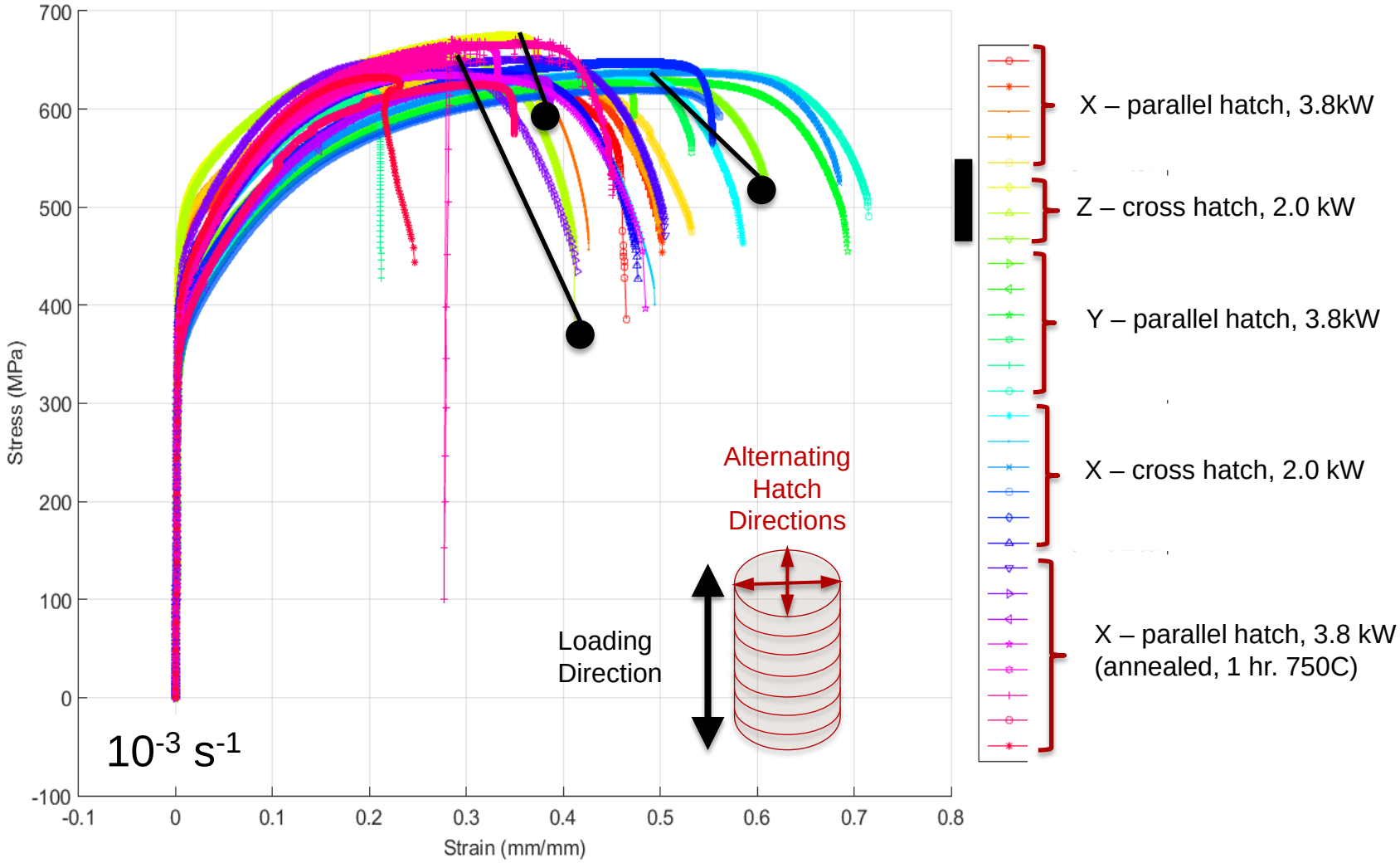

RS in Penn State AM Block using Hole Drilling Method

- High RS in AM samples
- Biaxial tensile RS
- Results **NOT** quantitative since stress > annealed yield stress of 316L

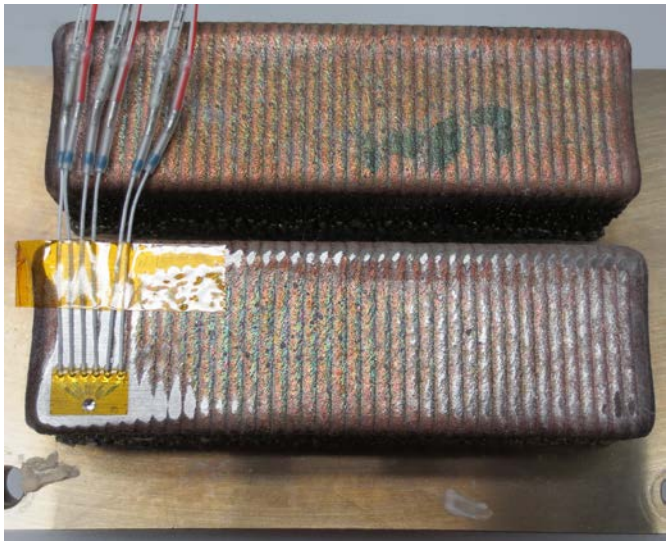

Sample courtesy of Mike Maguire

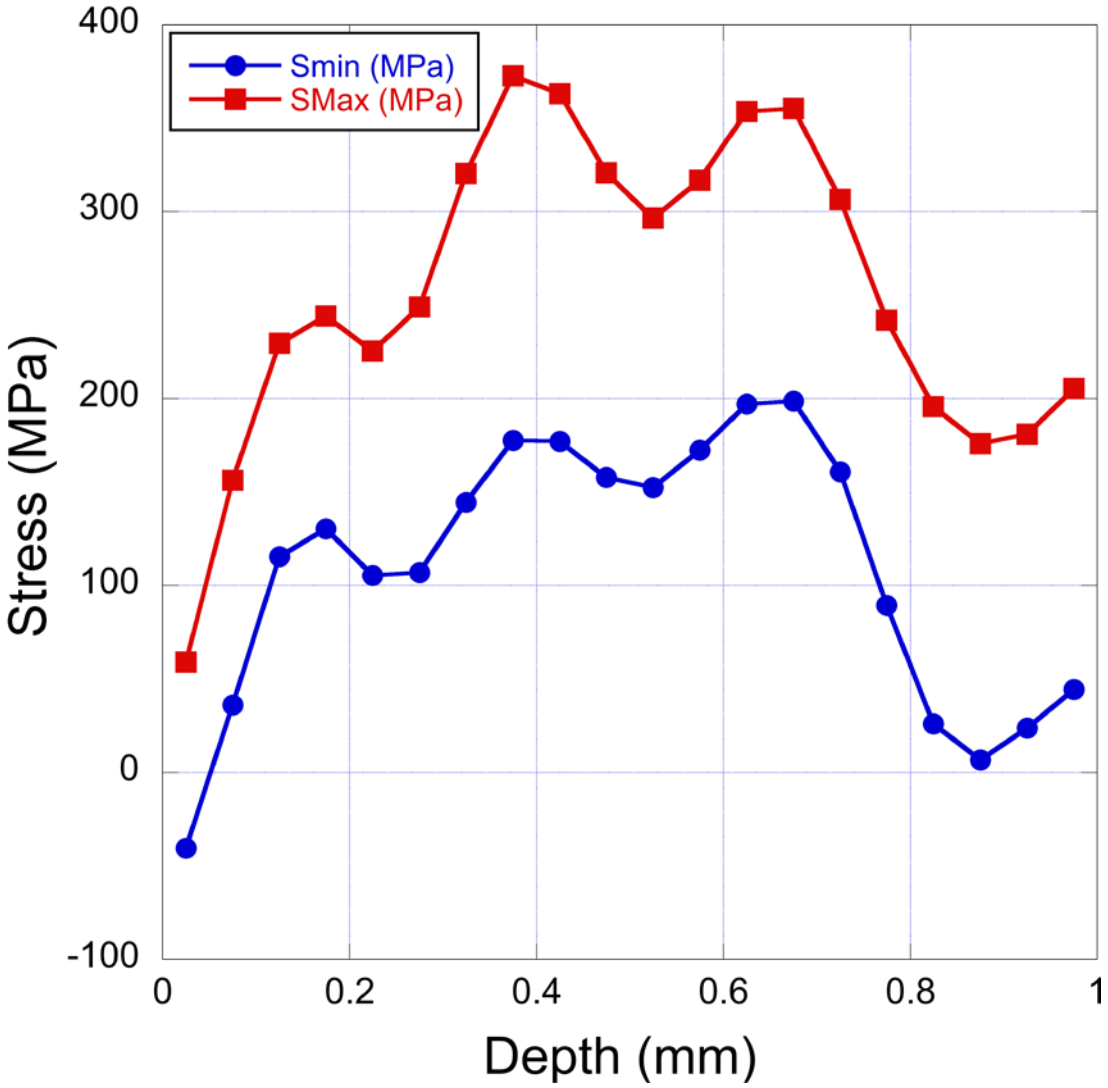

Primary Ferrite Solidification

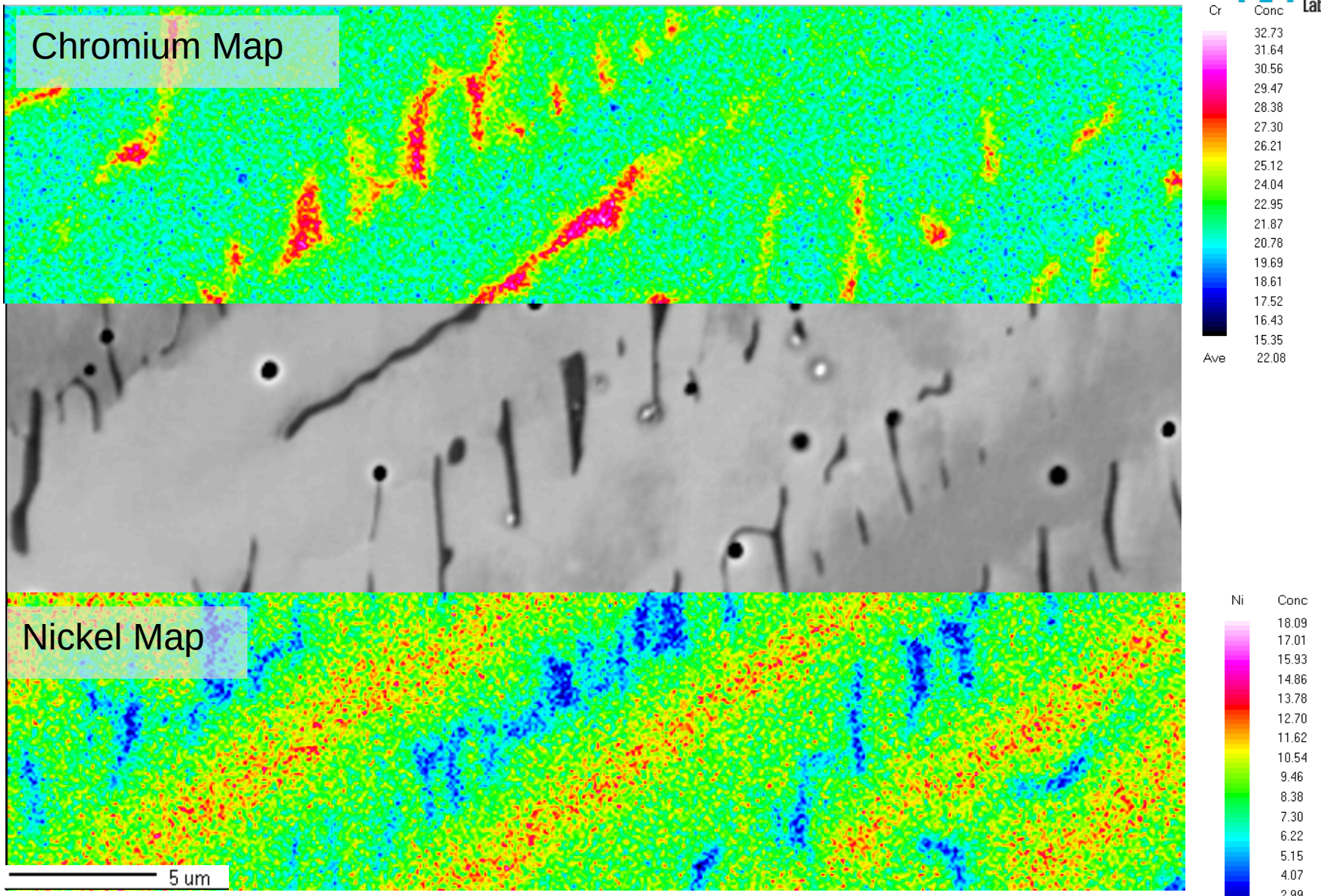

4.4 % Ferrite Locally

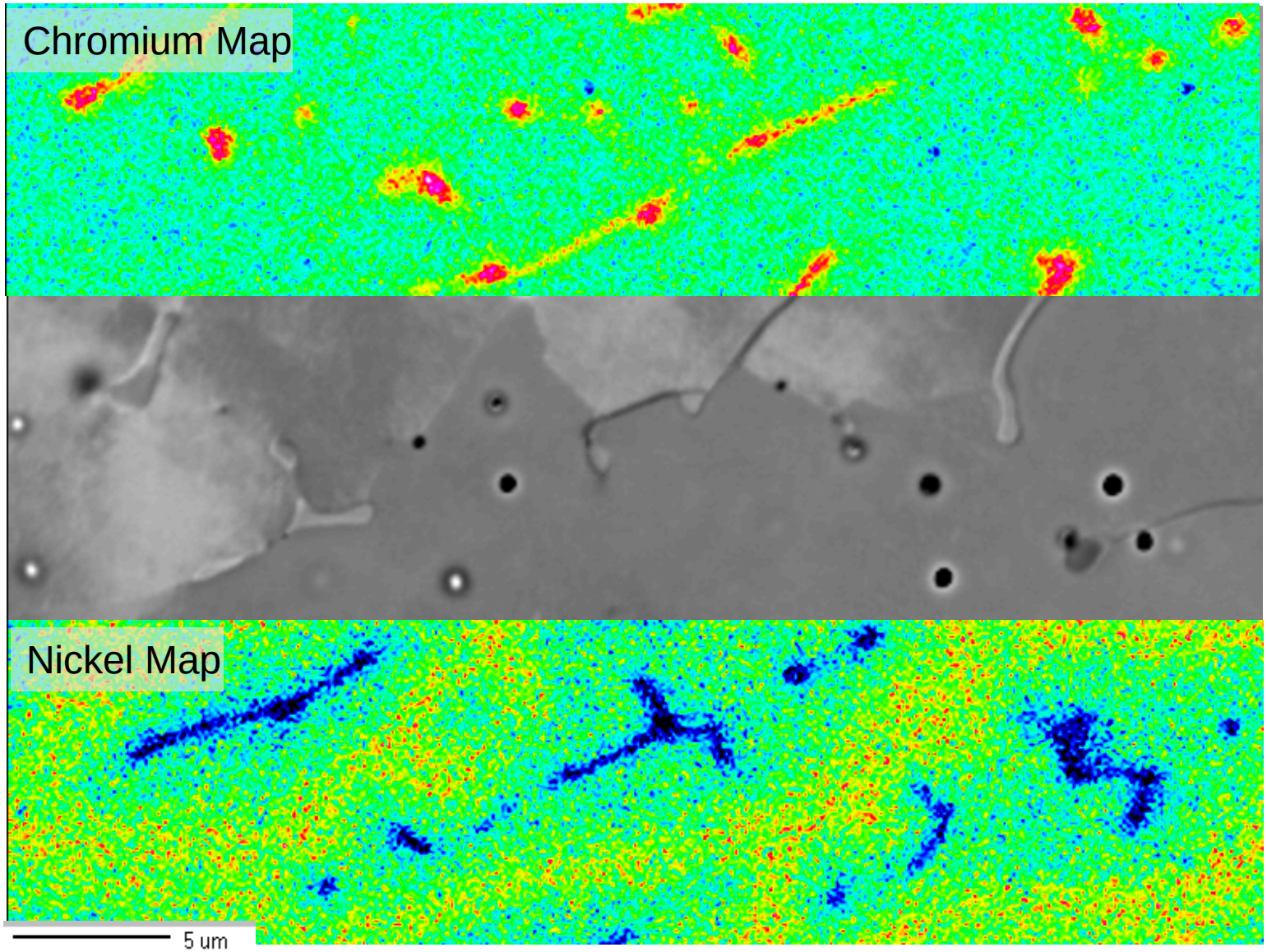

Sandia National Laboratories

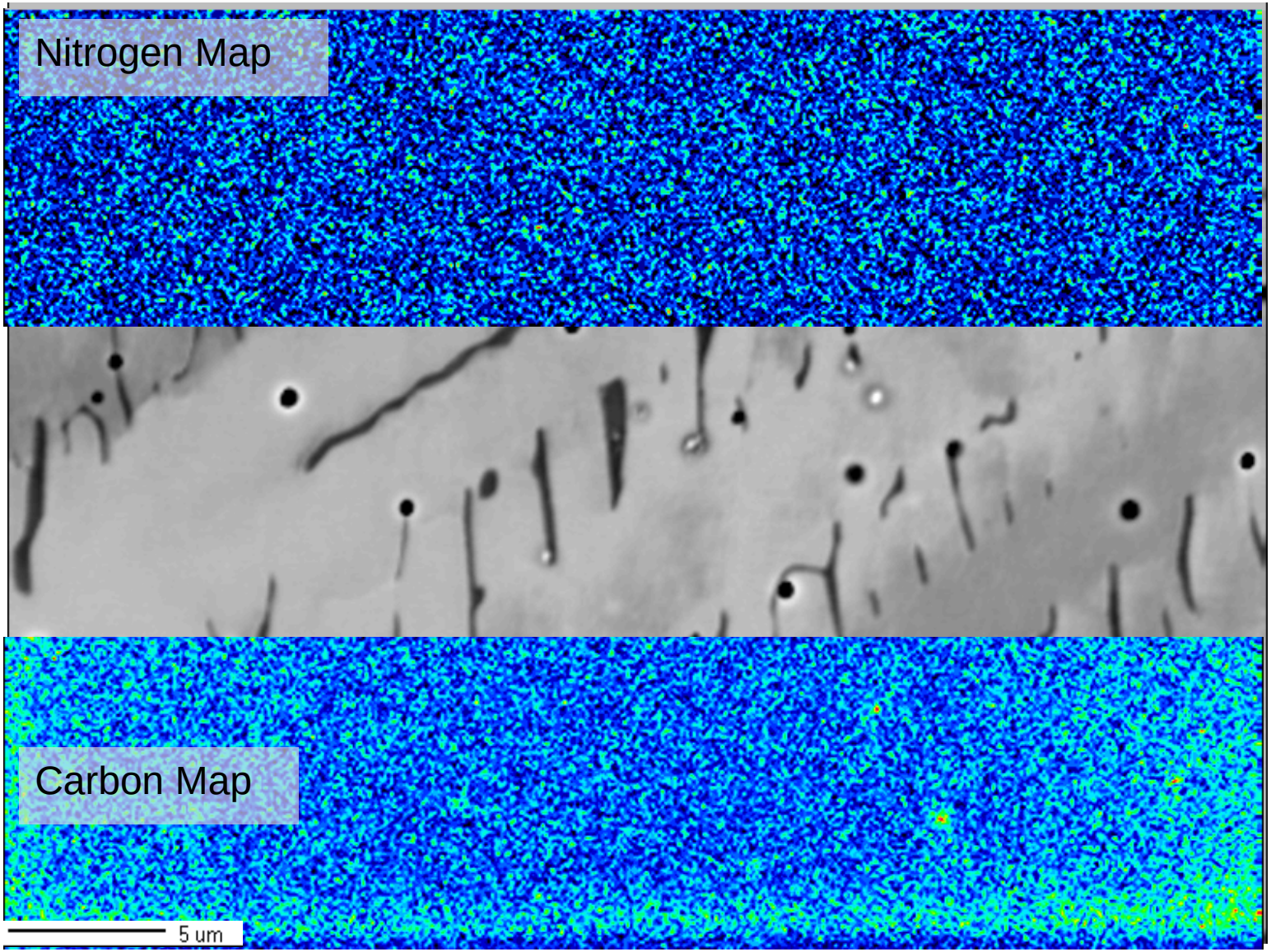
Nitrogen Map
Carbon Map
5 um

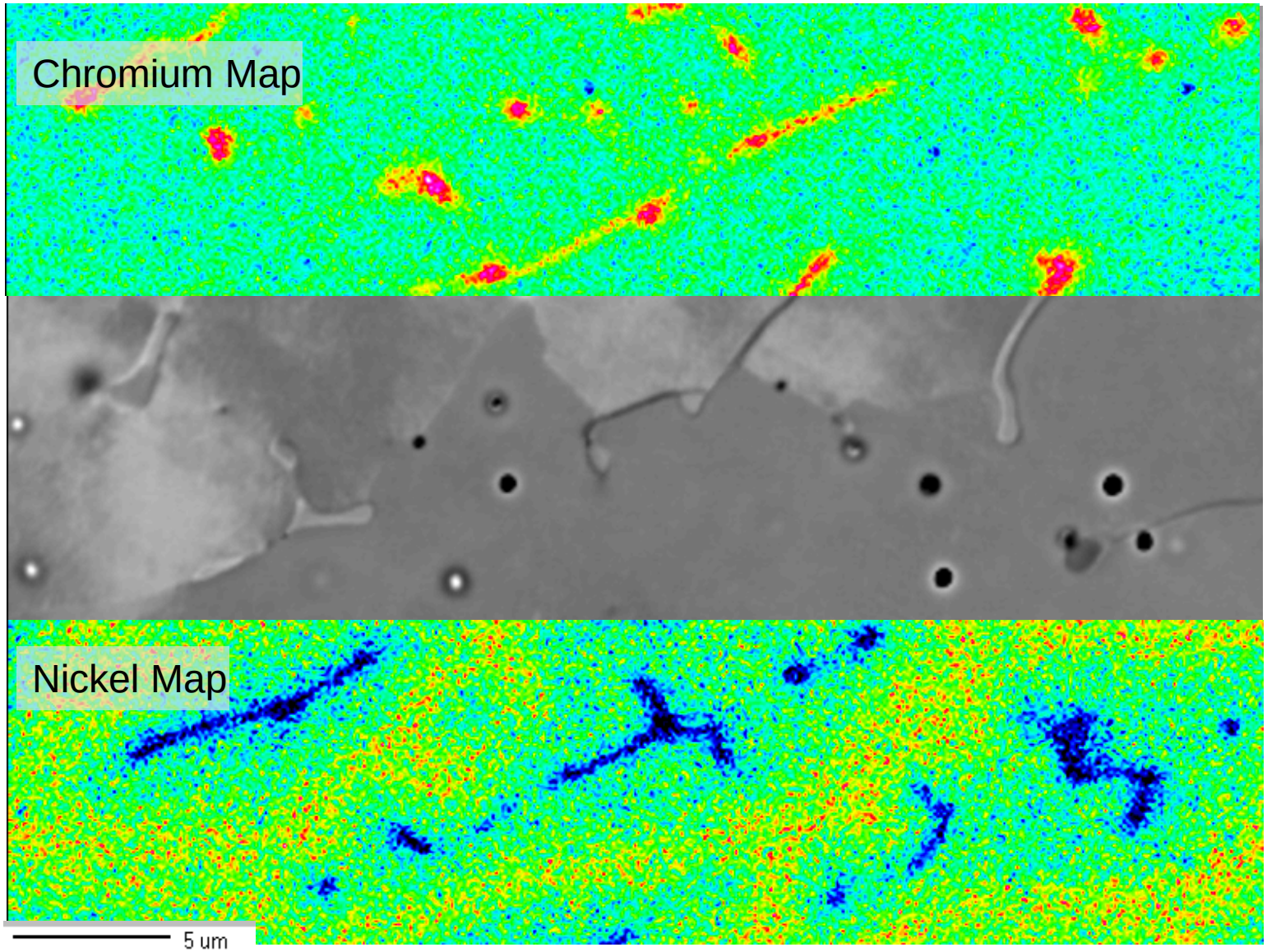

Sandia National Laboratories

Map 4